
Quantifying Differences in Reward Functions

Adam Gleave^{1*} Michael Dennis¹ Shane Legg² Stuart Russell¹ Jan Leike²
¹UC Berkeley ²DeepMind
gleave@berkeley.edu

Abstract

For many tasks, the reward function is too complex to be specified procedurally, and must instead be learned from user data. Prior work has evaluated learned reward functions by examining rollouts from a policy optimized for the learned reward. However, this method cannot distinguish between the learned reward function failing to reflect user preferences, and the reinforcement learning algorithm failing to optimize the learned reward. Moreover, the rollout method is highly sensitive to details of the environment the learned reward is evaluated in, which often differ in the deployment environment. To address these problems, we introduce the *Equivalent-Policy Invariant Comparison (EPIC)* distance to quantify the difference between two reward functions directly, without training a policy. We prove EPIC is invariant on an equivalence class of reward functions that always induce the same optimal policy. Furthermore, we find EPIC can be precisely approximated and is more robust than baselines to the choice of visitation distribution. Finally, we find that the EPIC distance of learned reward functions to the ground-truth reward is predictive of the success of training a policy, even in different transition dynamics.

1 Introduction

Reinforcement learning (RL) has reached or surpassed human performance in many domains with clearly-defined reward functions, such as games [26; 19; 28] and narrowly-scoped robotic manipulation tasks [20]. Unfortunately, the reward functions for most real-world tasks are difficult or impossible to procedurally specify. Even a task as simple as peg insertion from pixels has a non-trivial reward function that must usually be learned [27, IV.A]. Most real-world tasks have far more complex reward functions than this. In particular, tasks involving human interaction depend on complex and user-dependent preferences. These challenges have inspired work on learning a reward function, whether from demonstrations [17; 23; 31; 9; 4], preferences [1; 30; 7; 24; 32] or both [15; 5].

Prior work usually evaluates the learned reward function \hat{R} using the “rollout method”: training a policy $\pi_{\hat{R}}$ to optimize \hat{R} and then examining rollouts from $\pi_{\hat{R}}$. Unfortunately, this method is computationally expensive because it requires us to solve an RL problem. Furthermore, the rollout method produces *false negatives* when the reward \hat{R} matches user preferences, but the RL algorithm fails to maximize \hat{R} . The rollout method also produces *false positives*: of the many reward functions inducing the desired rollout in a given environment, only a small subset align with the user’s preferences. If the initial state distribution or transition dynamics change, misaligned rewards may induce undesirable policies.

For example, suppose a user likes apricots, tolerates plums and abhors durians. A reward function that prefers apricots to durians to plums induces the correct apricot-buying behavior at training time. But if the robot is shopping during an apricot shortage, it would buy a fruit the user hates: durians. A careful evaluation of the learned reward function before deployment should catch this error.

*Work partially conducted during an internship at DeepMind.

Table 1: Summary of the desiderata satisfied by each reward function distance. **Key** – the distance is: a *pseudometric* (section 3); *invariant* to potential shaping [18] and positive rescaling (section 3); a computationally *efficient* approximation achieving low error (section 6.1); *predictive* of the similarity of the trained policies (section 6.2); and *robust* to the choice of visitation distribution (section 6.3).

| Distance | Pseudometric | Invariant | Efficient | Predictive | Robust |
|----------|--------------|-----------|-----------|------------|--------|
| EPIC | ✓ | ✓ | ✓ | ✓ | ✓ |
| NPEC | ✗ | ✓ | ✗ | ✓ | ✗ |
| ERC | ✓ | ✗ | ✓ | ✓ | (✗) |

Reinforcement learning is founded on the observation that it is usually easier and more robust to specify a reward function, rather than a policy maximizing that reward function. Applying this insight to reward function analysis, we develop methods to compare reward functions *directly*, without training a policy. We summarize our desiderata for reward function distances in Table 1.

We introduce the *Equivalent-Policy Invariant Comparison (EPIC)* pseudometric that meets all five desiderata. EPIC (section 4) canonicalizes the reward functions’ potential-based shaping, then computes the correlation between the canonical rewards over a visitation distribution \mathcal{D} of transitions. For comparison, we also propose two baselines (section 5), *Episode Return Correlation (ERC)* and *Nearest Point in Equivalence Class (NPEC)*, which partially satisfy the desiderata.

EPIC works best when \mathcal{D} has support on all realistic transitions. In our experiments, we achieve this by using uninformative priors, such as a uniform distribution over transitions. Moreover, we find EPIC is robust to the exact choice of distribution \mathcal{D} , producing similar results across a range of distributions, whereas ERC and especially NPEC are highly sensitive to the choice of \mathcal{D} (section 6.3).

Reward learning algorithms are typically benchmarked on tasks with a known ground-truth reward function R . When using the rollout method, it is common to report the *regret*: how much less true reward R is obtained by a policy $\pi_{\hat{R}}$ optimized for the learned reward \hat{R} versus a policy π_R optimized for R . We find learned reward functions with low EPIC distance to the true reward R induce policies with low regret in both the training and an unseen test environment (section 6.2). Reward functions with high EPIC distance fail in the test environment but sometimes work in the training environment. EPIC therefore has a lower false positive rate than the rollout method, making it particularly attractive in safety-critical applications where reliability is a key design goal.

2 Related work

There exists a variety of methods to learn reward functions. One prominent family is inverse reinforcement learning (IRL; [17]), which infers a reward function from demonstrations. The IRL problem is inherently underconstrained: many different reward functions can lead to the same demonstrations. Bayesian IRL [23] handles this ambiguity by inferring a posterior over reward functions. By contrast, Maximum Entropy IRL [31] selects the highest entropy reward function consistent with the demonstrations; this method has scaled to high-dimensional environments [8; 9].

An alternative approach is to learn from *preference comparisons* between two trajectories [1; 30; 7; 24]. T-REX [5] is a hybrid approach, learning from a *ranked* set of demonstrations. More directly, Cabi et al. [6] learn from “sketches” of cumulative reward over an episode.

To the best of our knowledge, there is no prior work that focuses on evaluating reward functions directly. The most closely related work is Ng et al. [18], identifying reward transformations guaranteed not to change the optimal policy. However, a variety of ad-hoc methods have been developed to evaluate reward functions. The rollout method – evaluating rollouts of a policy trained on the learned reward – is evident in the earliest work on IRL [17]. Fu et al. [9] refined the rollout method by testing on a transfer environment, inspiring our experiment in section 6.2. Recent work has compared reward functions by scatterplotting returns [15; 5], inspiring our ERC baseline (section 5.1).

3 Background

This section introduces material needed for the distances defined in subsequent sections. We start by defining a distance *metric*, then introduce the *Markov Decision Process (MDP)* formalism, and finally describe when reward functions induce the same optimal policy in any compatible MDP.

Definition 3.1. Let X be a set and $d : X \times X \rightarrow [0, \infty)$ a function. d is a premetric if $d(x, x) = 0$ for all $x \in X$. d is a pseudometric if, furthermore, for all $x, y, z \in X$, $d(x, y) = d(y, x)$ and $d(x, z) \leq d(x, y) + d(y, z)$. d is a metric if, furthermore, for all $x, y \in X$, $d(x, y) = 0 \iff x = y$.

We wish for $d(R_A, R_B) = 0$ when reward functions R_A and R_B are in the same equivalence class, even if $R_A \neq R_B$. This is forbidden in a metric but permitted in a pseudometric, while retaining other guarantees such as symmetry and triangle inequality that a metric provides. Accordingly, a pseudometric is usually the best choice for a distance d over reward functions.

Definition 3.2. A Markov Decision Process (MDP) $M = (\mathcal{S}, \mathcal{A}, \gamma, \mu, \mathcal{T}, R)$ consists of a set of states \mathcal{S} and a set of actions \mathcal{A} ; a discount factor $\gamma \in [0, 1]$; an initial state distribution $\mu(s)$; a transition distribution $\mathcal{T}(s' | s, a)$ specifying the probability of transitioning to s' from s after taking action a ; and a reward function $R(s, a, s')$ specifying the reward upon taking action a in state s and transitioning to state s' .

A trajectory τ consists of a sequence of states and actions, $\tau = (s_0, a_0, s_1, a_1, \dots)$, where each $s_i \in \mathcal{S}$ and $a_i \in \mathcal{A}$. The *return* on a trajectory is defined as the sum of discounted rewards, $g(\tau; R) = \sum_{t=0}^{|\tau|-1} \gamma^t R(s_t, a_t, s_{t+1})$, where the length of the trajectory $|\tau|$ may be infinite.

In the following, we assume a discounted ($\gamma < 1$) infinite-horizon MDP. The results can be generalized to undiscounted ($\gamma = 1$) MDPs subject to regularity conditions needed for convergence.

A *stochastic policy* $\pi(a | s)$ assigns probabilities to taking action $a \in \mathcal{A}$ in state $s \in \mathcal{S}$. The objective of an MDP is to find a policy π that maximizes the expected return, $G(\pi) = \mathbb{E}_{\tau(\pi)} [g(\tau; R)]$, where $\tau(\pi)$ is a trajectory generated by sampling the initial state s_0 from μ , each action a_t from the policy $\pi(a_t | s_t)$ and successor states s_{t+1} from the transition distribution $\mathcal{T}(s_{t+1} | s_t, a_t)$. An MDP M has a set of optimal policies $\pi^*(M)$ that maximize the expected return, $\pi^*(M) = \arg \max_{\pi} G(\pi)$.

In this paper, we consider the setting where we only have access to an MDP $M^- = (\mathcal{S}, \mathcal{A}, \gamma, \mu, \mathcal{T})$. The unknown reward function R must be learned from human data. Typically, only the state space \mathcal{S} , action space \mathcal{A} and discount γ are known exactly, with the initial state μ and transition dynamics \mathcal{T} only observable from interacting with the environment M^- . In the following, we describe an equivalence class whose members are guaranteed to have the same set of optimal policies in any MDP M^- with fixed \mathcal{S} , \mathcal{A} and γ (allowing the unknown \mathcal{T} and μ to take arbitrary values).

Definition 3.3. A potential shaping reward is defined as $R(s, a, s') = \gamma\Phi(s') - \Phi(s)$, given a potential $\Phi : \mathcal{S} \rightarrow \mathbb{R}$ and where γ is the MDP discount rate.

Definition 3.4 (Reward Equivalence). We define two bounded reward functions R_A and R_B to be equivalent, $R_A \equiv R_B$, for a fixed $(\mathcal{S}, \mathcal{A}, \gamma)$ if and only if there exists a constant $\lambda > 0$ and a bounded potential function $\Phi : \mathcal{S} \rightarrow \mathbb{R}$ such that for all $s, s' \in \mathcal{S}$ and $a \in \mathcal{A}$:

$$R_B(s, a, s') = \lambda R_A(s, a, s') + \gamma\Phi(s') - \Phi(s).$$

Note $R_A - R_B \equiv \text{Zero}$ (where *Zero* is the all-zero reward) if and only if $R_A \equiv R_B$ with $\lambda = 1$.

Proposition 3.5. The binary relation \equiv is an equivalence relation. Let $R_A, R_B, R_C : \mathcal{S} \times \mathcal{A} \times \mathcal{S} \rightarrow \mathbb{R}$ be bounded reward functions. Then \equiv is reflexive, $R_A \equiv R_A$; symmetric, $R_A \equiv R_B$ implies $R_B \equiv R_A$; and transitive, $(R_A \equiv R_B) \wedge (R_B \equiv R_C)$ implies $R_A \equiv R_C$.

Proof. See section A.3.1 in supplementary material. □

The expected return of potential shaping $\gamma\Phi(s') - \Phi(s)$ on a trajectory segment (s_0, \dots, s_T) is $\gamma^T\Phi(s_T) - \Phi(s_0)$. The first term $\gamma^T\Phi(s_T) \rightarrow 0$ as $T \rightarrow \infty$, while the second term $\Phi(s_0)$ only depends on the initial state, and so potential shaping does not change the set of optimal policies [18].

Scaling a reward function by a positive factor $\lambda > 0$ scales the expected return of all trajectories by λ , leaving the set of optimal policies unchanged. The set of optimal policies is also invariant to a constant shift $c \in \mathbb{R}$ of the reward, however this can already be obtained by shifting Φ by $\frac{c}{\gamma-1}$.[†]

[†]Note constant shifts in the reward of an undiscounted MDP would cause the value function to diverge. Fortunately, the shaping $\gamma\Phi(s') - \Phi(s)$ is unchanged by constant shifts to Φ when $\gamma = 1$.

If $R_A \equiv R_B$, for a fixed $(\mathcal{S}, \mathcal{A}, \gamma)$, then for any MDP $M^- = (\mathcal{S}, \mathcal{A}, \gamma, \mu, \mathcal{T})$ we have $\pi^*((M^-, R_A)) = \pi^*((M^-, R_B))$, where (M^-, R) denotes the MDP specified by M^- with reward function R . In other words, R_A and R_B induce the same optimal policies for all initial state distributions μ and transition dynamics \mathcal{T} .

4 Comparing reward functions with EPIC

In this section we introduce the *Equivalent-Policy Invariant Comparison (EPIC)* pseudometric. This novel distance canonicalizes the reward functions' potential-based shaping, then compares the canonical representatives using Pearson distance, which is invariant to scale. Together, this construction makes EPIC invariant on reward equivalence classes. See section A.3.2 for proofs.

We define the *canonically shaped reward* $C_{\mathcal{D}_S, \mathcal{D}_A}(R)$ as an expectation over some arbitrary distributions \mathcal{D}_S and \mathcal{D}_A over states S and actions A respectively. This construction means $C_{\mathcal{D}_S, \mathcal{D}_A}(R)$ only depends on $(\mathcal{S}, \mathcal{A}, \gamma)$, and not on the initial state distribution μ or transition dynamics \mathcal{T} . In particular, no environment interaction is required to compute $C_{\mathcal{D}_S, \mathcal{D}_A}(R)$.

Definition 4.1 (Canonically Shaped Reward). *Let $R : \mathcal{S} \times \mathcal{A} \times \mathcal{S} \rightarrow \mathbb{R}$ be a reward function. Given distributions \mathcal{D}_S and \mathcal{D}_A over states S and actions A respectively, let S and S' be random variables independently sampled from \mathcal{D}_S and A sampled from \mathcal{D}_A . We define the canonically shaped R to be:*

$$C_{\mathcal{D}_S, \mathcal{D}_A}(R)(s, a, s') = R(s, a, s') + \mathbb{E}[\gamma R(s', A, S') - R(s, A, S') - \gamma R(S, A, S')].$$

Informally, if R' is shaped by potential Φ , then increasing $\Phi(s')$ increases $R'(s, a, s')$ by $\gamma\Phi(s')$ but decreases $\mathbb{E}[\gamma R'(s', A, S')]$ by $\gamma\Phi(s')$, canceling. Similarly increasing $\Phi(s)$ decreases $R'(s, a, s')$ but increases $\mathbb{E}[R'(s, A, S')]$. Finally, $\mathbb{E}[R(S, A, S')]$ centers the reward, canceling constant shift.

Proposition 4.2 (The Canonically Shaped Reward is Invariant to Shaping). *Let $R : \mathcal{S} \times \mathcal{A} \times \mathcal{S} \rightarrow \mathbb{R}$ be a reward function and $\Phi : \mathcal{S} \rightarrow \mathbb{R}$ a potential function. Let $\gamma \in [0, 1]$ be a discount rate, and \mathcal{D}_S and \mathcal{D}_A be distributions over states S and A respectively. Let R' denote R shaped by Φ : $R'(s, a, s') = R(s, a, s') + \gamma\Phi(s') - \Phi(s)$. Then the canonically shaped R' and R are equal: $C_{\mathcal{D}_S, \mathcal{D}_A}(R') = C_{\mathcal{D}_S, \mathcal{D}_A}(R)$.*

Proposition 4.2 holds for arbitrary distributions \mathcal{D}_S and \mathcal{D}_A . However, distributions with broad support over realistic states and actions produce more stable canonical transformations. Specifically, we would like for small changes in the input reward to produce small changes in the canonical representative. That is, letting ϵ be a small noise term, $C_{\mathcal{D}_S, \mathcal{D}_A}(R + \epsilon) \approx C_{\mathcal{D}_S, \mathcal{D}_A}(R)$.

Viewing R as a real vector, $C_{\mathcal{D}_S, \mathcal{D}_A}(R)$ is a linear transformation with coefficients given by the joint distribution for $S \times A \times S'$. This transformation is most stable when the coefficients are uniform, so we favor distributions with broad support in our experiments. However, sometimes it is appropriate to place less weight on certain states and actions, e.g. if they're known to be physically unreachable.

So far, we have removed any dependence on potential shaping. We must still normalize the scale of rewards, and then compare the normalized rewards. The Pearson distance does this in a single step.

Definition 4.3. *The Pearson distance between random variables X and Y is defined by the expression $D_\rho(X, Y) = \frac{1}{\sqrt{2}}\sqrt{1 - \rho(X, Y)}$, where $\rho(X, Y)$ is the Pearson correlation between X and Y .*

Lemma 4.4. *The Pearson distance D_ρ is a pseudometric.*

Lemma 4.5. *Let $a, b \in (0, \infty)$, $c, d \in \mathbb{R}$ and X, Y be random variables. Then it follows that $0 \leq D_\rho(aX + c, bY + d) = D_\rho(X, Y) \leq 1$.*

We can now define EPIC in terms of the Pearson distance between canonically shaped rewards.

Definition 4.6 (Equivalent-Policy Invariant Comparison (EPIC) pseudometric). *Let \mathcal{D} be some visitation distribution over transitions $s \xrightarrow{a} s'$. Let S, A, S' be random variables jointly sampled from \mathcal{D} . Let \mathcal{D}_S and \mathcal{D}_A be some distributions over states S and A respectively. The Equivalent-Policy Invariant Comparison (EPIC) distance between reward functions R_A and R_B is the Pearson distance between their canonically shaped versions over \mathcal{D} :*

$$D_{\text{EPIC}}(R_A, R_B) = D_\rho(C_{\mathcal{D}_S, \mathcal{D}_A}(R_A)(S, A, S'), C_{\mathcal{D}_S, \mathcal{D}_A}(R_B)(S, A, S')).$$

Theorem 4.7. *The Equivalent-Policy Invariant Comparison distance is a pseudometric.*

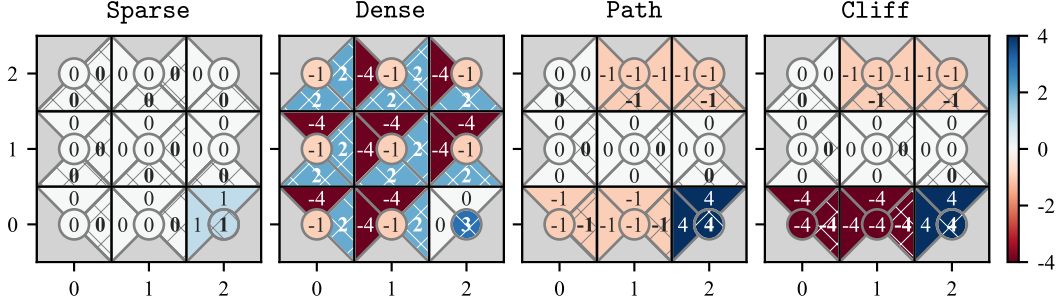


Figure 1: Heatmaps of reward functions $R(s, a, s')$ for a deterministic 3×3 gridworld. $R(s, \text{stay}, s)$ is given by the central circle in cell s . $R(s, a, s')$ is given by the triangular wedge in cell s adjacent to cell s' in direction a . Optimal action(s) (for infinite horizon, discount $\gamma = 0.99$) have bold labels against a hatched background. See figure A.2 for the distances between all reward pairs.

EPIC is invariant to potential shaping and positive affine transformations, and so is invariant on \equiv .

Theorem 4.8. Let $R_A, R'_A, R_B, R'_B : \mathcal{S} \times \mathcal{A} \times \mathcal{S} \rightarrow \mathbb{R}$ be reward functions such that $R'_A \equiv R_A$ and $R'_B \equiv R_B$. Then $0 \leq D_{\text{EPIC}}(R'_A, R'_B) = D_{\text{EPIC}}(R_A, R_B) \leq 1$.

As a pedagogical example, we compute the EPIC distance between the reward functions in figure 1 for a deterministic 3×3 gridworld. Despite assigning different rewards to each transition, Sparse and Dense are equivalent and have zero EPIC distance. By contrast, $D_{\text{EPIC}}(\text{Path}, \text{Cliff}) = 0.27$, almost as much as $D_{\text{EPIC}}(\text{Sparse}, \text{Cliff}) = 0.37$. Although Path and Cliff have identical optimal policies in deterministic settings, the rewards induce very different optimal policies under stochastic dynamics. See figure A.2 for the distances between all reward pairs.

We choose state and action distributions $\mathcal{D}_{\mathcal{S}}$ and $\mathcal{D}_{\mathcal{A}}$ uniform over \mathcal{S} and \mathcal{A} , and visitation distribution $\mathcal{D}_{\text{unif}}$ uniform over state-action pairs (s, a) , with s' deterministically computed. It is important these distributions have adequate support. As an extreme example, if $\mathcal{D}_{\mathcal{S}}$ and $\mathcal{D}_{\text{unif}}$ have no support for a particular state then the reward of that state has no effect on the distance. We can compute EPIC exactly in a tabular setting, but in general must use a sample-based approximation (section A.1.1).

5 Baseline approaches for comparing reward functions

To the best of our knowledge, EPIC is the first method to quantitatively evaluate reward functions without training a policy. Given the lack of established methods, we develop two alternatives as baselines: Episode Return Correlation (ERC) and Nearest Point in Equivalence Class (NPEC).

5.1 Episode Return Correlation (ERC)

The goal of an MDP is to maximize expected episode return, so it is natural to compare reward functions by the returns they induce. If the return of a reward function R_A is a positive affine transformation of another reward R_B , then R_A and R_B have the same set of optimal policies. This suggests using Pearson distance, which is invariant to positive affine transformations.

Definition 5.1 (Episode Return Correlation (ERC) pseudometric). Let \mathcal{D} be some distribution over trajectories. Let E be a random variable sampled from \mathcal{D} . The Episode Return Correlation distance between reward functions R_A and R_B is the Pearson distance between their episode returns on \mathcal{D} , $D_{\text{ERC}}(R_A, R_B) = D_{\rho}(g(E; R_A), g(E; R_B))$.

Prior work has scatterplot the return of R_A against R_B over episodes [5, figure 3] and fixed-length segments [15, section D]. ERC is the Pearson distance of such plots, so is a natural baseline. We approximate ERC by the correlation of episode returns on a finite collection of rollouts.

Under special conditions, ERC is invariant to shaping. Let R be a reward function and Φ a potential function, and define the shaped reward $R'(s, a, s') = R(s, a, s') + \gamma\Phi(s') - \Phi(s)$. The return under the shaped reward on a trajectory $\tau = (s_0, a_0, \dots, s_T)$ is $g(\tau; R') = g(\tau; R) + \gamma^T\Phi(s_T) - \Phi(s_0)$.

If the initial state s_0 and terminal state s_T are fixed, then $\gamma^T \Phi(s_T) - \Phi(s_0)$ is constant. Since Pearson distance is invariant to constant shifts, ERC is invariant to shaping in this case. For infinite-horizon discounted MDPs, only the initial state s_0 need be fixed, since $\gamma^T \Phi(s_T) \rightarrow 0$ as $T \rightarrow \infty$.

However, if the initial state s_0 is stochastic, the ERC distance can take on arbitrary values under shaping. Let R_A and R_B be two arbitrary reward functions. Suppose that there are at least two distinct initial states, s_A and s_B , with non-zero measure in \mathcal{D} . Choose potential $\Phi(s) = 0$ everywhere except $\Phi(s_A) = \Phi(s_B) = c$, and let R'_A and R'_B denote R_A and R_B shaped by Φ . As $c \rightarrow \infty$, the correlation $\rho(g(E; R'_A), g(E; R'_B))$ tends to one. This is since the relative difference tends to zero, even though $g(E; R'_A)$ and $g(E; R'_B)$ continue to have the same absolute difference as c varies. Consequently, the ERC pseudometric $D_{\text{ERC}}(R'_A, R'_B) \rightarrow 0$ as $c \rightarrow \infty$. By an analogous argument, setting $\Phi(s_A) = c$ and $\Phi(s_B) = -c$ gives $D_{\text{ERC}}(R'_A, R'_B) \rightarrow 1$ as $c \rightarrow \infty$.

5.2 Nearest Point in Equivalence Class (NPEC)

NPEC takes the minimum L^p distance between equivalence classes. See section A.3.3 for proofs.

Definition 5.2 (L^p distance). *Let \mathcal{D} be a visitation distribution over transitions $s \xrightarrow{a} s'$ and let $p \geq 1$ be a power. The L^p distance between reward functions R_A and R_B is the L^p norm of their difference:*

$$D_{L^p}(R_A, R_B) = \left(\mathbb{E}_{s,a,s' \sim \mathcal{D}} [|R_A(s, a, s') - R_B(s, a, s')|^p] \right)^{1/p}.$$

Proposition 5.3. (1) D_{L^p} is a metric in L^p space, where functions f and g are identified if $f = g$ almost everywhere on \mathcal{D} . (2) It is a pseudometric when f and g are identified if $f = g$ at all points.

The L^p distance is sensitive to shaping and positive rescaling that do not change the optimal policy. A natural solution is to take the distance from the *nearest point* in the equivalence class. The *Unnormalized Nearest Point in Equivalence Class* distance is: $D_{\text{NPEC}}^U(R_A, R_B) = \inf_{R'_A \equiv R_A} D_{L^p}(R'_A, R_B)$.

Note the infimum over *both* $R'_A \equiv R_A$ and $R'_B \equiv R_B$ would always be zero, since all equivalence classes come arbitrarily close to the origin in L^p space. However, taking the infimum over only $R'_A \equiv R_A$ causes $D_{\text{NPEC}}^U(R_A, R_B)$ to be sensitive to the scale of R_B . We fix this by normalizing.

Definition 5.4. *The Nearest Point in Equivalence Class (NPEC) premetric is defined by:*

$$D_{\text{NPEC}}(R_A, R_B) = \frac{D_{\text{NPEC}}^U(R_A, R_B)}{D_{\text{NPEC}}^U(\text{Zero}, R_B)} \text{ when } D_{\text{NPEC}}^U(\text{Zero}, R_B) \neq 0 \text{ and } 0 \text{ otherwise.}$$

Note if $D_{\text{NPEC}}^U(\text{Zero}, R_B) = 0$ then $D_{\text{NPEC}}^U(R_A, R_B) = 0$ since R_A can be scaled arbitrarily close to Zero . Since all policies are optimal for $\bar{R} \equiv \text{Zero}$, we choose $D_{\text{NPEC}}(R_A, R_B) = 0$ in this case.

Proposition 5.5. D_{NPEC} is a premetric.

Note that D_{NPEC} is *not* in general a pseudometric: see proposition A.1 for a counterexample. It is, however, bounded and invariant to shaping, similar to EPIC.

Theorem 5.6. *Let $R_A, R'_A, R_B, R'_B : \mathcal{S} \times \mathcal{A} \times \mathcal{S} \rightarrow \mathbb{R}$ be reward functions such that $R_A \equiv R'_A$ and $R_B \equiv R'_B$. Then $0 \leq D_{\text{NPEC}}(R'_A, R'_B) = D_{\text{NPEC}}(R_A, R_B) \leq 1$.*

The infimum in D_{NPEC}^U can be computed exactly in a tabular setting, but in general we must approximate it using gradient descent. This gives an upper bound for D_{NPEC}^U , but the quotient of upper bounds D_{NPEC} may be too low or too high. See section A.1.2 for details of the approximation.

6 Experiments

We evaluate EPIC and the baselines ERC and NPEC in a variety of continuous control tasks. First, we compute the distance between hand-designed reward functions, finding EPIC to be the most reliable distance. Although NPEC produces qualitatively similar results, it has a high degree of approximation error. Moreover, ERC sometimes suffers from pathological failures, such as assigning a high distance to equivalent rewards. Second, we find the distance of learned reward functions to a ground-truth reward predicts the return obtained by policy training, even in an unseen test environment. Finally, we show EPIC is robust to the exact choice of visitation distribution \mathcal{D} , whereas ERC and especially NPEC are highly sensitive to the choice of \mathcal{D} .

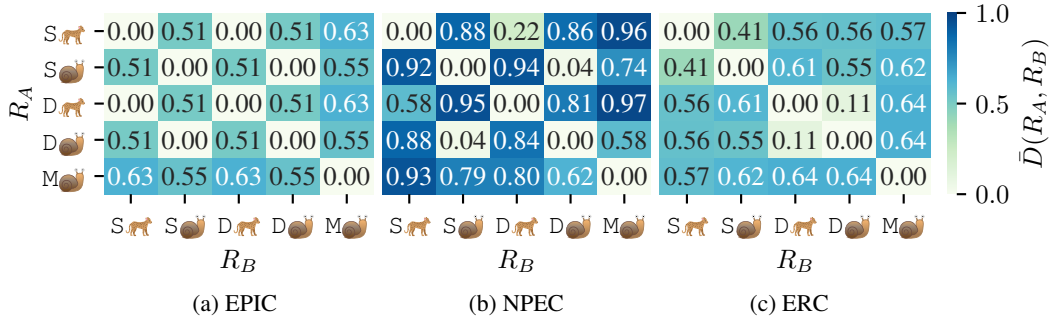


Figure 2: Approximate distances between hand-designed reward functions in PointMass. The visitation distribution \mathcal{D} is sampled from rollouts of a policy π_{unif} taking actions uniformly at random. **Key:** 🐘 quadratic control penalty, 🐘 no control penalty. S is $\text{Sparse}(x) = \mathbb{1}[|x| < 0.05]$, D is shaped $\text{Dense}(x, x') = \text{Sparse}(x) + |x'| - |x|$, while M is $\text{Magnitude}(x) = -|x|$. Width of 95% confidence interval (see Figure A.3) is less than 0.02 for EPIC and ERC but as large as 0.3 for NPEC.

6.1 Comparing hand-designed reward functions

We compare procedurally specified reward functions in four tasks. Figure 2 presents results in the proof-of-concept PointMass task. The results for Gridworld, HalfCheetah and Hopper, in section A.2.4, are qualitatively similar. In PointMass the agent can accelerate left or right on a line. The reward functions include (🐘) or exclude (🐘) a quadratic penalty $\|a\|_2^2$. The sparse reward (S) gives a reward of 1 in the region around the goal state. The dense reward (D) is a shaped version of the sparse reward. The magnitude reward (M) is the negative distance of the agent from the goal.

We find that EPIC correctly identifies the equivalent reward pairs (S 🐘-D 🐘 and S 🐘-D 🐘) with estimated distance $< 1 \times 10^{-3}$. By contrast, NPEC suffers from considerable approximation error: $D_{\text{NPEC}}(\text{D 🐘}, \text{S 🐘}) = 0.58$. Similarly, ERC’s erroneous handling of shaping when the initial state is stochastic produces $D_{\text{ERC}}(\text{D 🐘}, \text{S 🐘}) = 0.56$. In the next section, we compare learned rewards.

6.2 Predicting policy performance from reward distance

We train reward models on the PointMaze task from Fu et al. [9], and evaluate the ground-truth (GT) return of a policy optimized for the learned reward. Table 2 shows that rewards with low distance from GT achieve high returns. Rewards with high distance sometimes work but are context sensitive.

PointMaze is a MuJoCo environment where a point mass agent must navigate around a wall to reach a goal. The *train* and *test* variants differ only in the position of the wall. We evaluate four reward learning algorithms: Regression onto reward labels [*target* method from 7, section 3.3], Preference comparisons on trajectories [7], and adversarial IRL with a state-only (AIRL SO) and state-action (AIRL SA) reward model [9]. All models are trained using synthetic data from an oracle with access to the ground-truth; see section A.2.2 for details.

Both *Regress* and *Pref* achieve very low distances, producing near-expert policy performance in both the *train* and *test* variants. The AIRL SO and AIRL SA models have distances an order of magnitude greater. The more expressive AIRL SA achieves near-expert performance in *train* but fails to transfer to *test*. The less-expressive AIRL SO has poor performance in both variants, although the generator policy (trained simultaneously with the reward) performs reasonably in *train*.

Due to reward ambiguity, rewards such as AIRL * that are distant from the ground-truth GT can still produce a good policy. For example, a “memorized” reward function that assigns reward only to states visited by an expert will induce the expert policy in the *train* variant. Nonetheless, it will have a large distance from GT, even if the visitation distribution \mathcal{D} only contains transitions from *train*. This is appropriate since in *test* the “expert” policy produced by this reward runs straight into the wall.

6.3 Sensitivity of reward distance to visitation state distribution

We would like the reward distances to be robust to the exact choice of visitation distribution \mathcal{D} . In Table 2, we report distances calculated under distributions induced by rollouts from three different

Table 2: Distances of reward models from ground-truth (GT), and the mean GT return of policies optimized from-scratch for the reward model in the *train* and *test* variants of PointMaze. We also report returns for AIRL’s *generator* policy, jointly trained with the reward. Distances ($1000\times$ scale) use visitation distribution \mathcal{D} from rollouts in the *train* environment of: a uniform random policy π_{unif} , an expert π^* and a **Mixture** of these policies. \mathcal{D}_S and \mathcal{D}_A are computed by marginalizing \mathcal{D} . 95% confidence intervals (see Table A.6) are tighter than $\pm 1\%$ for EPIC and ERC but are as large as $\pm 50\%$ for NPEC due to high variance across seeds.

| Reward Model | $1000 \times D_{\text{EPIC}}$ | | | $1000 \times D_{\text{NPEC}}$ | | | $1000 \times D_{\text{ERC}}$ | | | Episode Return | | |
|-----------------|-------------------------------|---------|------|-------------------------------|---------|-------|------------------------------|---------|------|----------------|-------|-------|
| | π_{unif} | π^* | Mix | π_{unif} | π^* | Mix | π_{unif} | π^* | Mix | Gen. | Train | Test |
| GT | 0 | 0 | 0 | 0 | 0 | 0 | 0 | 0 | 0 | — | −5.99 | −6.05 |
| Regress | 41.9 | 36.5 | 25.9 | 0.519 | 14.9 | 0.140 | 4.78 | 40.9 | 1.39 | — | −6.99 | −6.51 |
| Pref | 50.5 | 54.4 | 32.9 | 2.99 | 204 | 1.78 | 15.0 | 180 | 8.15 | — | −6.62 | −7.02 |
| AIRL S0 | 488 | 600 | 395 | 684 | 3550 | 426 | 448 | 382 | 234 | −9.44 | −28.5 | −11.7 |
| AIRL SA | 548 | 614 | 390 | 823 | 3030 | 376 | 506 | 467 | 208 | −6.69 | −6.91 | −28.5 |

policies. π_{unif} takes actions uniformly at random, producing broad support over transitions; π^* is an expert policy, yielding a distribution concentrated at or near the goal; and **Mix** is a mixture of the two.

We find EPIC is robust to varying \mathcal{D} : the distance varies by less than $2\times$, and the ranking between the reward models is the same across visitation distributions, except for **Mix** favoring AIRL SA over AIRL S0. By contrast, NPEC is highly sensitive to the choice of \mathcal{D} : the distance of Pref varies by over $500\times$ between π_{unif} and π^* . ERC lies somewhere in the middle: the distances vary by as much as $25\times$. Overall, EPIC is clearly the least sensitive to choice of \mathcal{D} in this environment.

Nonetheless, even with EPIC some care must be taken when choosing \mathcal{D} . Typically, \mathcal{D} is collected via rollouts of some exploration policy in an environment. This works well when the deployment environment has a similar set of reachable states to the rollout environment, even if some details of the dynamics – such as the position of the wall in PointMaze – differ. However, when the deployment environment allows a transition (s, a, s') that is not physically attainable in the rollout environment, then \mathcal{D} will place no support on this transition and the reward $R(s, a, s')$ can take arbitrary values without affecting the distance. In general, any black-box method for assessing reward models – including the rollout method – only has predictive power on transitions that it visits during testing.

7 Discussion

Our novel EPIC distance compares reward functions directly, without training a policy. We have proved it satisfies the axioms of a pseudometric, and moreover is bounded and invariant to equivalent rewards. Empirically, we find the EPIC distance between procedurally specified reward functions is more reliable than the NPEC and ERC baselines.

Furthermore, we find the distance of learned reward functions to the ground-truth reward predicts the return of policies optimized for the learned reward, in both the *train* and unseen *test* environments. This is important since it is common for the initial state distribution or transition dynamics to change between the training environment where the reward function was learned, and the test environment where the system is deployed [22; 2; 21]. For example, one might learn a reward and policy in simulation, and then fine-tune the policy in the real world with the learned reward.

An important direction for future work is to evaluate reward models trained on noisy and biased human data. Such models will have a higher EPIC distance from the ground-truth than models trained on synthetic data, however some algorithms may be more robust to imperfect feedback than others.

Benchmarks are an important driver of progress in machine learning. Unfortunately, traditional policy-based metrics do not provide any guarantees as to the fidelity of the learned reward function. We believe the EPIC distance will be a highly informative addition to the evaluation toolbox, and would encourage researchers to report EPIC distance in addition to policy-based metrics.

Broader Impact

Reinforcement learning (RL) is used to choose push notifications to send to billions of users [10], and in the coming years we are likely to see more large-scale deployment of RL systems in interactive applications. This gives renewed urgency to specifying an appropriate objective for these systems to optimize. Even with the best of intentions, designers cannot possibly anticipate the desires of all their users, let alone procedurally specify this. In the absence of better methods, engineers often resort to proxies such as user engagement. While such metrics are often correlated with user satisfaction, Goodhart’s law predicts this correlation will break down when used as an optimization objective [12]. This can lead to negative unintended consequences, such as addiction to online platforms.

A natural alternative is to instead learn the reward function from user feedback. This democratizes AI systems: rather than the designer picking an optimization objective, the users choose how they wish the AI system to interact with them. The system could even learn a reward function for each user, and optimize that objective on an individual basis (subject to some global fairness constraints).

However, current reward learning algorithms have considerable limitations. We believe quantifying differences in reward functions will help improve benchmarking of reward learning algorithms, spurring algorithmic improvements. Additionally, we anticipate it to be useful as a verification method prior to deployment of a learned reward model.

The main potential downside we see from our work is if people place too much trust in the reward distances proposed in this paper. While we are confident the distance between reward functions will be a highly informative addition to the set of available evaluation metrics, it is intended as a complement and not a replacement for other forms of testing. In particular, it will continue to be important to test the trained policy prior to deployment, especially in safety-critical systems. Even if the learned reward function is correct, there is no guarantee that the policy behaves as desired – for example, policies often suffer from adversarial examples [14; 11].

References

- [1] Riad Akrou, Marc Schoenauer, and Michele Sebag. Preference-based policy learning. In *Machine Learning and Knowledge Discovery in Databases*, 2011.
- [2] Dario Amodei, Chris Olah, Jacob Steinhardt, Paul F. Christiano, John Schulman, and Dan Mané. Concrete problems in AI safety. arXiv: 1606.06565v2 [cs.AI], 2016.
- [3] Dario Amodei, Paul Christiano, and Alex Ray. Learning from human preferences, June 2017. URL <https://openai.com/blog/deep-reinforcement-learning-from-human-preferences/>.
- [4] Dzmitry Bahdanau, Felix Hill, Jan Leike, Edward Hughes, Arian Hosseini, Pushmeet Kohli, and Edward Grefenstette. Learning to understand goal specifications by modelling reward. In *ICLR*, 2019.
- [5] Daniel S. Brown, Wonjoon Goo, Prabhat Nagarajan, and Scott Niekum. Extrapolating beyond suboptimal demonstrations via inverse reinforcement learning from observations. In *ICML*, 2019.
- [6] Serkan Cabi, Sergio Gómez Colmenarejo, Alexander Novikov, Ksenia Konyushkova, Scott Reed, Rae Jeong, Konrad Zolna, Yusuf Aytar, David Budden, Mel Vecerik, Oleg Sushkov, David Barker, Jonathan Scholz, Misha Denil, Nando de Freitas, and Ziyu Wang. Scaling data-driven robotics with reward sketching and batch reinforcement learning. arXiv: 1909.12200v2 [cs.RO], 2019.
- [7] Paul F Christiano, Jan Leike, Tom Brown, Miljan Martic, Shane Legg, and Dario Amodei. Deep reinforcement learning from human preferences. In *NIPS*, pages 4299–4307, 2017.
- [8] Chelsea Finn, Sergey Levine, and Pieter Abbeel. Guided cost learning: Deep inverse optimal control via policy optimization. In *ICML*, 2016.
- [9] Justin Fu, Katie Luo, and Sergey Levine. Learning robust rewards with adversarial inverse reinforcement learning. In *ICLR*, 2018.

- [10] Jason Gauci, Edoardo Conti, Yitao Liang, Kittipat Virochsiri, Yuchen He, Zachary Kaden, Vivek Narayanan, Xiaohui Ye, Zhengxing Chen, and Scott Fujimoto. Horizon: Facebook’s open source applied reinforcement learning platform. arXiv: 1811.00260 [cs.LG], 2018.
- [11] Adam Gleave, Michael Dennis, Cody Wild, Neel Kant, Sergey Levine, and Stuart Russell. Adversarial policies: Attacking deep reinforcement learning. In *ICLR*, 2020.
- [12] C. A. E. Goodhart. Problems of monetary management: the UK experience. In *Monetary Theory and Practice*, pages 91–121. Springer, 1984.
- [13] Ashley Hill, Antonin Raffin, Maximilian Ernestus, Adam Gleave, Anssi Kanervisto, Rene Traore, Prafulla Dhariwal, Christopher Hesse, Oleg Klimov, Alex Nichol, Matthias Plappert, Alec Radford, John Schulman, Szymon Sidor, and Yuhuai Wu. Stable Baselines. <https://github.com/hill-a/stable-baselines>, 2018.
- [14] Sandy H. Huang, Nicolas Papernot, Ian J. Goodfellow, Yan Duan, and Pieter Abbeel. Adversarial attacks on neural network policies. arXiv:1702.02284v1 [cs.LG], 2017.
- [15] Borja Ibarz, Jan Leike, Tobias Pohlen, Geoffrey Irving, Shane Legg, and Dario Amodei. Reward learning from human preferences and demonstrations in Atari. In *NeurIPS*, pages 8011–8023, 2018.
- [16] Charles L. Lawson and Richard J. Hanson. *Solving Least Squares Problems*. SIAM, 1995.
- [17] Andrew Y. Ng and Stuart Russell. Algorithms for inverse reinforcement learning. In *ICML*, 2000.
- [18] Andrew Y. Ng, Daishi Harada, and Stuart Russell. Policy invariance under reward transformations: theory and application to reward shaping. In *NIPS*, 1999.
- [19] OpenAI. OpenAI Five. <https://blog.openai.com/openai-five/>, 2018.
- [20] OpenAI, Ilge Akkaya, Marcin Andrychowicz, Maciek Chociej, Mateusz Litwin, Bob McGrew, Arthur Petron, Alex Paino, Matthias Plappert, Glenn Powell, Raphael Ribas, Jonas Schneider, Nikolas Tezak, Jerry Tworek, Peter Welinder, Lilian Weng, Qiming Yuan, Wojciech Zaremba, and Lei Zhang. Solving Rubik’s Cube with a robot hand. arXiv: 1910.07113v1 [cs.LG], 2019.
- [21] Xue Bin Peng, Marcin Andrychowicz, Wojciech Zaremba, and Pieter Abbeel. Sim-to-real transfer of robotic control with dynamics randomization. In *ICRA*, pages 3803–3810, 2018.
- [22] Joaquin Quiñero-Candela, Masashi Sugiyama, Anton Schwaighofer, and Neil D. Lawrence, editors. *Dataset Shift in Machine Learning*. MIT Press, 2008.
- [23] Deepak Ramachandran and Eyal Amir. Bayesian inverse reinforcement learning. In *IJCAI*, 2007.
- [24] Dorsa Sadigh, Anca D. Dragan, S. Shankar Sastry, and Sanjit A. Seshia. Active preference-based learning of reward functions. In *RSS*, July 2017.
- [25] John Schulman, Filip Wolski, Prafulla Dhariwal, Alec Radford, and Oleg Klimov. Proximal policy optimization algorithms. arXiv:1707.06347v2 [cs.LG], 2017.
- [26] David Silver, Aja Huang, Chris J. Maddison, Arthur Guez, Laurent Sifre, George van den Driessche, Julian Schrittwieser, Ioannis Antonoglou, Veda Panneershelvam, Marc Lanctot, Sander Dieleman, Dominik Grewe, John Nham, Nal Kalchbrenner, Ilya Sutskever, Timothy Lillicrap, Madeleine Leach, Koray Kavukcuoglu, Thore Graepel, and Demis Hassabis. Mastering the game of Go with deep neural networks and tree search. *Nature*, 529(7587):484–489, 2016.
- [27] Mel Vecerik, Oleg Sushkov, David Barker, Thomas Rothörl, Todd Hester, and Jon Scholz. A practical approach to insertion with variable socket position using deep reinforcement learning. In *ICRA*, 2019.

- [28] Oriol Vinyals, Igor Babuschkin, Wojciech M. Czarnecki, Michaël Mathieu, Andrew Dudzik, Junyoung Chung, David H. Choi, Richard Powell, Timo Ewalds, Petko Georgiev, Junhyuk Oh, Dan Horgan, Manuel Kroiss, Ivo Danihelka, Aja Huang, Laurent Sifre, Trevor Cai, John P. Agapiou, Max Jaderberg, Alexander S. Vezhnevets, Rémi Leblond, Tobias Pohlen, Valentin Dalibard, David Budden, Yury Sulsky, James Molloy, Tom L. Paine, Caglar Gulcehre, Ziyu Wang, Tobias Pfaff, Yuhuai Wu, Roman Ring, Dani Yogatama, Dario Wünsch, Katrina McKinney, Oliver Smith, Tom Schaul, Timothy Lillicrap, Koray Kavukcuoglu, Demis Hassabis, Chris Apps, and David Silver. Grandmaster level in StarCraft II using multi-agent reinforcement learning. *Nature*, 575(7782):350–354, 2019.
- [29] Steven Wang, Adam Gleave, and Sam Toyer. imitation: implementations of inverse reinforcement learning and imitation learning algorithms. <https://github.com/humancompatibleai/imitation>, 2020.
- [30] Aaron Wilson, Alan Fern, and Prasad Tadepalli. A Bayesian approach for policy learning from trajectory preference queries. In *NIPS*, 2012.
- [31] Brian D. Ziebart, Andrew Maas, J. Andrew Bagnell, and Anind K. Dey. Maximum entropy inverse reinforcement learning. In *AAAI*, 2008.
- [32] Daniel M. Ziegler, Nisan Stiennon, Jeffrey Wu, Tom B. Brown, Alec Radford, Dario Amodei, Paul Christiano, and Geoffrey Irving. Fine-tuning language models from human preferences. arXiv: 1909.08593v2 [cs.CL], 2019.

A Supplementary material

A.1 Approximation Procedures

A.1.1 Sample-based approximation for EPIC distance

We approximate EPIC distance (definition 4.6) using a sample-based approach. Specifically, we sample a batch B_V of N_V samples from the visitation distribution \mathcal{D} , and a batch B_M of N_M samples from the joint state and action distributions $\mathcal{D}_S \times \mathcal{D}_A$. We approximate the canonically shaped rewards (definition 4.1) by taking the mean over B_M :

$$\begin{aligned} C_{\mathcal{D}_S, \mathcal{D}_A}(R)(s, a, s') &= R(s, a, s') + \mathbb{E}[\gamma R(s', A, S') - R(s, A, S') - \gamma R(S, A, S')] \\ &\approx R(s, a, s') + \frac{\gamma}{N_M} \sum_{(x, u) \in B_M} R(s', u, x) \\ &\quad - \frac{1}{N_M} \sum_{(x, u) \in N_M} R(s, u, x) \\ &\quad - \frac{\gamma}{N_M^2} \sum_{(x, \cdot) \in B_M} \sum_{(x', u) \in B_M} R(x, u, x'). \end{aligned}$$

We then compute the Pearson distance between the approximate canonically shaped rewards on the batch of samples B_V .

A.1.2 Optimization-based approximation for NPEC distance

$D_{\text{NPEC}}(R_A, R_B)$ (section 5.2) is defined as the infimum of L^p distance over an infinite set of equivalent reward functions $R \equiv R_A$. We approximate this using gradient descent on the reward model:

$$R_{\nu, c, w}(s, a, s') = \exp(\nu) R_A(s, a, s') + c + \gamma \Phi_w(s') - \Phi_w(s),$$

where $\nu, c \in \mathbb{R}$ are scalar weights and w is a vector of weights parameterizing a deep neural network Φ_w . The constant $c \in \mathbb{R}$ is unnecessary if Φ_w has a bias term, but its inclusion simplifies the optimization problem.

We optimize ν, c, w to minimize the mean of the cost $J(\nu, c, w) = D(R_{\nu, c, w}(s, a, s'), R_B(s, a, s'))$ on samples (s, a, s') from a visitation distribution \mathcal{D} . Note the mean cost upper bounds the true NPEC distance since $R_{\nu, c, w} \equiv R_A$.

We found empirically that ν and c need to be initialized close to their optimal values for gradient descent to reliably converge. To resolve this problem, we initialize the affine parameters to $\nu \leftarrow \log \lambda$ and c found by:

$$\arg \min_{\lambda \geq 0, c \in \mathbb{R}} \mathbb{E}_{s, a, s' \sim \mathcal{D}} (\lambda R_A(s, a, s') + c - R_B(s, a, s'))^2.$$

We use the active set method of Lawson and Hanson [16] to solve this constrained least-squares problem. These initial affine parameters minimize the L^p distance $D_{L^p}(R_{\nu, c, 0}(s, a, s'), R_B(s, a, s'))$ under the metric $\ell(x, y) = (x - y)^2$ with the potential fixed at $\Phi_0(s) = 0$.

A.1.3 Confidence Intervals

We report confidence intervals to help measure the degree of error introduced by the approximation. Since approximate distances may not be normally distributed, we use bootstrapping to produce a distribution-free confidence interval. For EPIC and NPEC, we compute independent approximate distances over different seeds, and then compute a bootstrapped confidence interval on the distances for each seed. We use 30 seeds for EPIC but only 3 seeds for NPEC due to its greater computational requirements. In ERC, computing the distance is very cheap, so we instead apply bootstrapping to the collected *episodes*, computing the ERC distance for each bootstrapped episode sample.

A.2 Experiments

A.2.1 Hyperparameters for Approximate Distances

Table A.1 summarizes the hyperparameters and distributions used to compute the distances between reward functions. Most parameters are the same across all environments. We use a visitation distribution of uniform random transitions $\mathcal{D}_{\text{unif}}$ in the simple GridWorld environment with known deterministic dynamics. In other environments, the visitation distribution is sampled from rollouts

Table A.1: Summary of hyperparameters and distributions used in experiments. The uniform random visitation distribution $\mathcal{D}_{\text{unif}}$ samples states and actions uniformly at random, and samples the next state from the transition dynamics. Random policy π_{unif} takes uniform random actions. The synthetic expert policy π^* was trained with PPO on the ground-truth reward. **Mixture** samples actions from either π_{unif} or π^* , switching between them at each timestep with probability 0.05. Warmstart Size is the size of the dataset used to compute initialization parameters described in section A.1.2.

| Parameter | Value | In experiment |
|---------------------------------------|--|--------------------------------|
| Visitation Distribution \mathcal{D} | Random transitions $\mathcal{D}_{\text{unif}}$ | GridWorld |
| | Rollouts from π_{unif} | PointMass, HalfCheetah, Hopper |
| | π_{unif} , π^* and Mixture | PointMaze |
| Bootstrap Samples | 10 000 | All |
| Discount γ | 0.99 | All |
| EPIC | | |
| State Distribution \mathcal{D}_S | $N(0, 1)$ standard Gaussian | PointMass, HalfCheetah, Hopper |
| | Marginalized from \mathcal{D} | PointMaze |
| Action Distribution \mathcal{D}_A | $U[-1, 1]$ continuous uniform | PointMass, HalfCheetah, Hopper |
| | Marginalized from \mathcal{D} | PointMaze |
| Seeds | 30 | All |
| Samples N_V | 32 768 | All |
| Mean Samples N_M | 32 768 | All |
| NPEC | | |
| Seeds | 3 | All |
| Total Timesteps | 1×10^6 | All |
| Optimizer | Adam | All |
| Learning Rate | 1×10^{-2} | All |
| Batch Size | 4096 | All |
| Warmstart Size | 16 386 | All |
| Loss ℓ | $\ell(x, y) = (x - y)^2$ | All |
| ERC | | |
| Episodes | 131 072 | All |

of a policy. We use a random policy π_{unif} for PointMass, HalfCheetah and Hopper in the hand-designed reward experiments (section 6.1). In PointMaze, we compare three visitation distributions (section 6.3) induced by rollouts of π_{unif} , an expert policy π^* and a **Mixture** of the two policies, sampling actions from either π_{unif} or π^* and switching between them with probability 0.05 per timestep.

A.2.2 Training Learned Reward Models

For the experiments on learned reward functions (sections 6.2 and 6.3), we trained reward models using adversarial inverse reinforcement learning (AIRL; 9), preference comparison [7] and by regression onto the ground-truth reward [*target* method from 7, section 3.3]. For AIRL, we use an existing open-source implementation [29]. We developed new implementations for preference comparison and regression, available at — double blind: supplementary material —. We also use the RL algorithm proximal policy optimization (PPO; 25) on the ground-truth reward to train expert policies to provide demonstrations for AIRL, and on learned reward models to evaluate their performance.

For PPO and AIRL we used the default hyperparameters in tables A.2 and A.3, finding them adequate and so performing no further tuning. For preference comparison we performed a sweep over batch size, trajectory length and learning rate to decide on the hyperparameters in table A.4. Total timesteps was selected once diminishing returns were observed in loss curves. The exact value of the regularization weight was found to be unimportant, largely controlling the scale of the output at convergence. Finally, for regression we performed a sweep over batch size, learning rate and total timesteps to decide on the hyperparameters in table A.5. We found batch size and learning rate to

Table A.2: Hyperparameters for proximal policy optimisation (PPO) [25]. We used the implementation and default hyperparameters from Hill et al. [13]. PPO was used to train expert policies on ground-truth reward and to optimize learned reward functions for evaluation.

| Parameter | Value | In environment |
|-----------------------------|----------------------|----------------|
| Total Timesteps | 1×10^6 | All |
| Batch Size | 16 384 | PointMaze |
| | 1024 | All others |
| Discount γ | 0.99 | |
| Entropy Coefficient | 0.01 | |
| Learning Rate | 2.5×10^{-4} | |
| Value Function Coefficient | 0.5 | |
| Gradient Clipping Threshold | 0.5 | |
| Ratio Clipping Threshold | 0.2 | |
| Lambda (GAE) | 0.95 | |
| Minibatches | 4 | |
| Optimization Epochs | 4 | |
| Parallel Environments | 8 | |

Table A.3: Hyperparameters for adversarial inverse reinforcement learning (AIRL) used in Wang et al. [29].

| Parameter | Value |
|---------------------------------|--------------------------------|
| RL Algorithm | PPO [25] |
| Total Timesteps | 102 400 |
| Discount γ | 0.99 |
| Demonstration Timesteps | 100 000 |
| Generator Batch Size | 2048 |
| Discriminator Batch Size | 50 |
| Entropy Weight | 1.0 |
| Reward Function Architecture | MLP, two 32-unit hidden layers |
| Potential Function Architecture | MLP, two 32-unit hidden layers |

Table A.4: Hyperparameters for preference comparison used in our implementation of Christiano et al. [7].

| Parameter | Value | Range Tested |
|---------------------------------|--------------------------------|--|
| Total Timesteps | 5×10^6 | $[1, 10 \times 10^6]$ |
| Batch Size | 10 000 | $[500, 250\ 000]$ |
| Trajectory Length | 5 | $[1, 100]$ |
| Learning Rate | 1×10^{-2} | $[1 \times 10^{-4}, 1 \times 10^{-1}]$ |
| Discount γ | 0.99 | |
| Reward Function Architecture | MLP, two 32-unit hidden layers | |
| Output L2 Regularization Weight | 1×10^{-4} | |

Table A.5: Hyperparameters for regression used in our implementation of Christiano et al. [7, *target* method from section 3.3].

| Parameter | Value | Range Tested |
|------------------------------|--------------------------------|--|
| Total Timesteps | 10×10^6 | $[1, 20 \times 10^6]$ |
| Batch Size | 4096 | $[256, 16\ 384]$ |
| Learning Rate | 2×10^{-2} | $[1 \times 10^{-3}, 1 \times 10^{-1}]$ |
| Discount γ | 0.99 | |
| Reward Function Architecture | MLP, two 32-unit hidden layers | |

be relatively unimportant with many combinations performing well, but regression was found to converge slowly but steadily requiring a relatively large 10×10^6 timesteps for good performance in our environments.

All algorithms are trained on synthetic data generated from the ground-truth reward function. AIRL is provided with a large demonstration dataset of 100 000 timesteps from an expert policy trained on the ground-truth reward, similar in size to the total number of timesteps AIRL is trained for (see table A.3). In preference comparison and regression, each batch is sampled afresh from the visitation distribution specified in table A.1 and labeled according to the ground-truth reward.

A.2.3 Computing infrastructure

Experiments were conducted on a small number of `n1-standard-96` Google Cloud Platform VM instances, with 48 CPU cores on an Intel Skylake processor and 360 GB of RAM. It takes less than a week of compute on a single `n1-standard-96` instance to run all the experiments described in this paper.

A.2.4 Comparing hand-designed reward functions

We compute distances between hand-designed reward functions in four environments: `GridWorld`, `PointMass`, `HalfCheetah` and `Hopper`. The reward functions for `GridWorld` are described in Figure A.1, and the distances are reported in Figure A.2. We report the approximate distances and confidence intervals between reward functions in the other environments in Figures A.3, A.4 and A.5.

We find the (approximate) EPIC distance closely matches our intuitions for similarity between the reward functions. NPEC often produces similar results to EPIC, but unfortunately is dogged by optimization error. This is particularly notable in higher-dimensional environments like `HalfCheetah` and `Hopper`, where the NPEC distance often exceeds the theoretical upper bound of 1.0 and the confidence interval width is frequently larger than 0.2.

By contrast, ERC distance generally has a tight confidence interval, but systematically fails in the presence of shaping. For example, it confidently assigns large distances between *equivalent* reward pairs in `PointMass` such as `S🐘-D🐘`. However, ERC produces reasonable results in `HalfCheetah` and `Hopper` where rewards are all similarly shaped. In fact, ERC picks up on a detail in `Hopper` that EPIC misses: whereas EPIC assigns a distance of around 0.71 between all rewards of different types (running vs backflipping), ERC assigns lower distances when the rewards are in the same direction (forward or backward). Given this, ERC may be attractive in some circumstances, especially given the ease of implementation. However, we would caution against using it in isolation due to the likelihood of misleading results in the presence of shaping.

A.2.5 Comparing learned reward functions

Previously, we reported the mean approximate distance from a ground-truth reward of four learned reward models in `PointMaze` (Table 2). Since these distances are approximate, we report 95% lower and upper bounds computed via bootstrapping in Table A.6. We also include the relative difference of the upper and lower bounds from the mean, finding the relative difference to be fairly consistent across reward models for a given algorithm and visitation distribution pair. The relative difference is less than 1% for all EPIC and ERC distances. However, NPEC confidence intervals can be as wide as 50%: this is due to the method’s high variance, and the small number of seeds we were able to run because of the method’s computational expense.

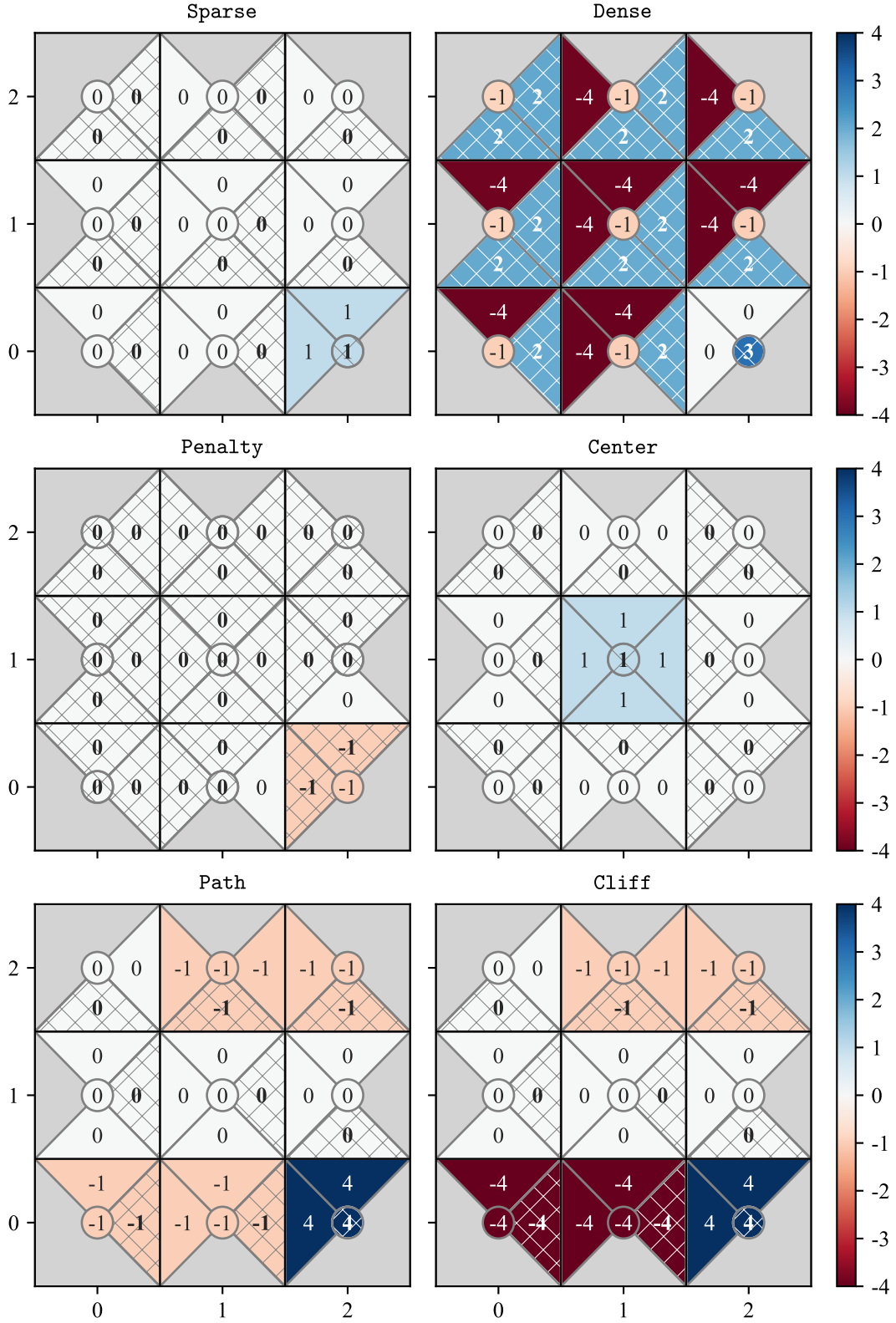
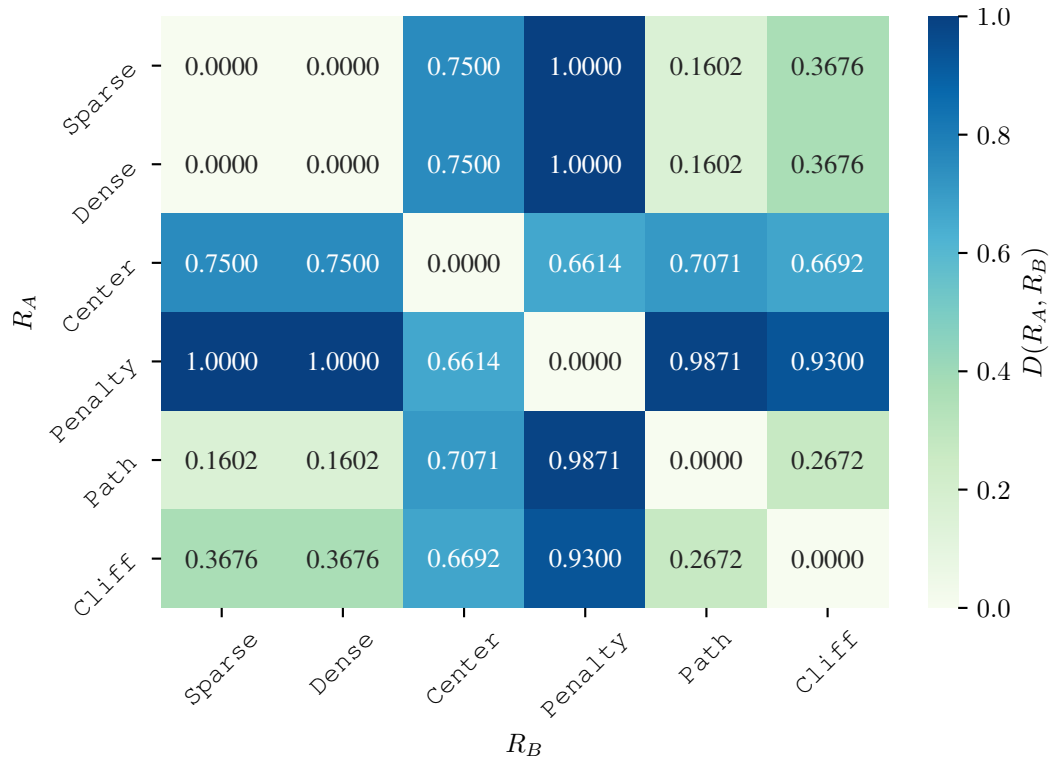
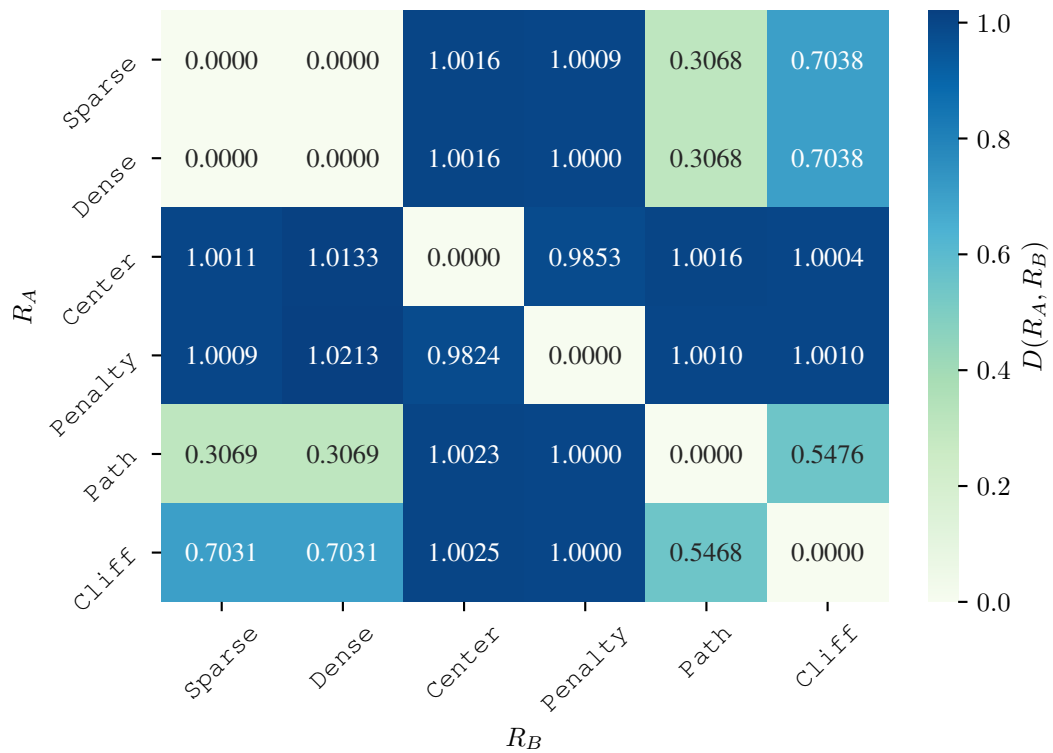


Figure A.1: Heatmaps of reward functions $R(s, a, s')$ for a 3×3 deterministic gridworld. $R(s, \text{stay}, s)$ is given by the central circle in cell s . $R(s, a, s')$ is given by the triangular wedge in cell s adjacent to cell s' in direction a . Optimal action(s) (for infinite horizon, discount $\gamma = 0.99$) have bold labels against a hatched background. See figure A.2 for the distance between all reward pairs.



(a) EPIC



(b) NPEC

Figure A.2: Distances between hand-designed reward functions for the 3×3 deterministic Gridworld environment. See figure A.1 for definitions of each reward. Distances are computed using tabular algorithms. We do not report confidence intervals since these algorithms are deterministic and exact up to floating point error.

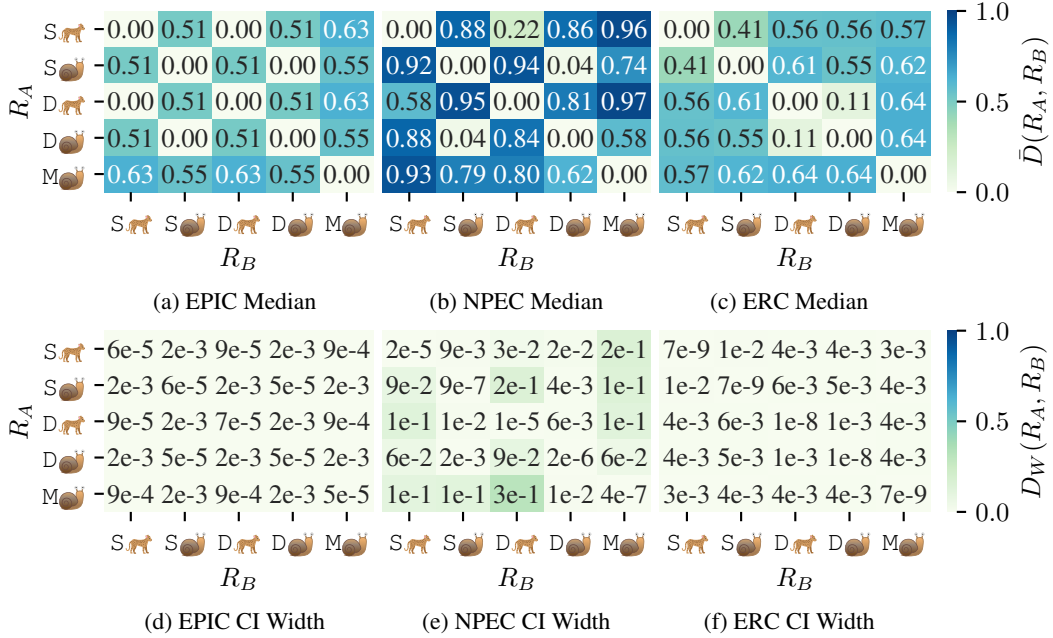


Figure A.3: Approximate distances between hand-designed reward functions in PointMass. The visitation distribution \mathcal{D} is sampled from rollouts of a policy π_{unif} taking actions uniformly at random. **Key:** 🐶 quadratic control penalty, 🐕 no control penalty. S is Sparse(x) = $\mathbb{1}[|x| < 0.05]$, D is shaped Dense(x, x') = Sparse(x) + $|x'| - |x|$, while M is Magnitude(x) = $-|x|$. **Confidence Interval (CI):** 95% CI computed by bootstrapping over 10 000 samples.

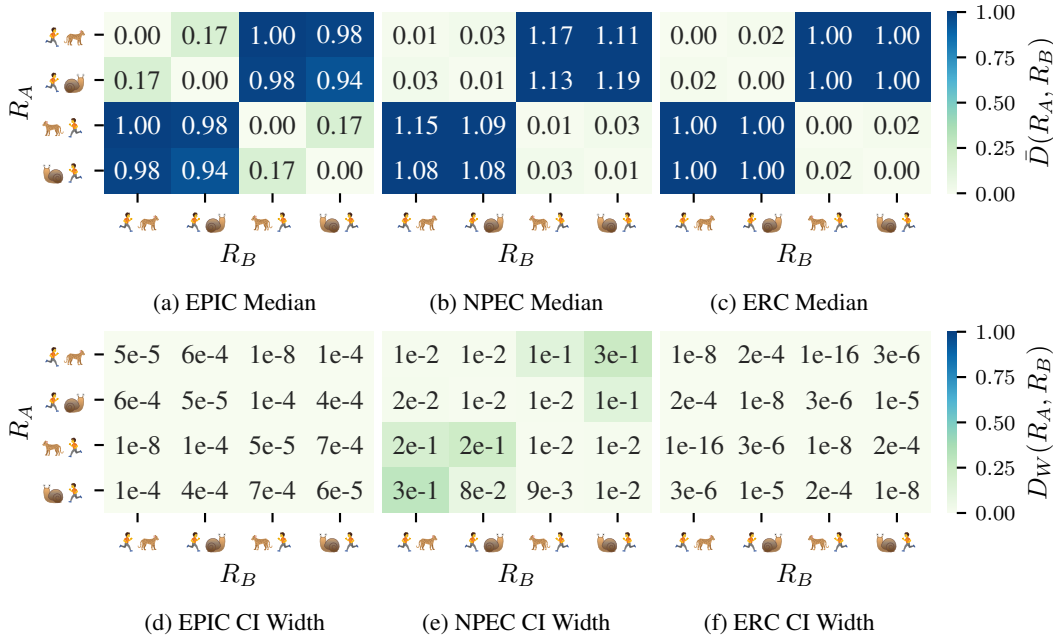


Figure A.4: Approximate distances between hand-designed reward functions in HalfCheetah. The visitation distribution \mathcal{D} is sampled from rollouts of a policy π_{unif} taking actions uniformly at random. **Key:** 🏃 is a reward proportional to the change in center of mass and moving *forward* is rewarded when 🏃 to the right, and moving *backward* is rewarded when 🏃 to the left. 🐶 quadratic control penalty, 🐕 no control penalty. **Confidence Interval (CI):** 95% CI computed by bootstrapping over 10 000 samples.

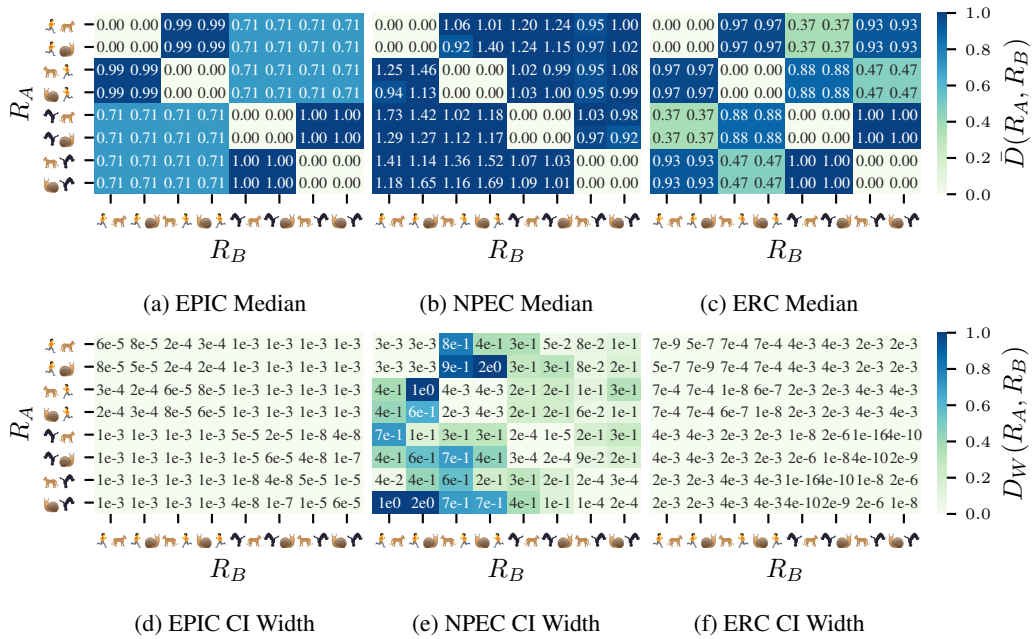


Figure A.5: Approximate distances between hand-designed reward functions in Hopper. The visitation distribution \mathcal{D} is sampled from rollouts of a policy π_{unif} taking actions uniformly at random. **Key:** 🏃 is a reward proportional to the change in center of mass and 🤸 is the backflip reward defined in Amodei et al. [3, footnote]. Moving *forward* is rewarded when 🏃 or 🤸 is to the right, and moving *backward* is rewarded when 🏃 or 🤸 is to the left. 🐼 quadratic control penalty, 🐾 no control penalty. **Confidence Interval (CI):** 95% CI computed by bootstrapping over 10 000 samples.

Table A.6: Approximate distances of learned reward models from the ground-truth (GT). We report the 95% bootstrapped lower and upper bounds, the mean, and a 95% bound on the relative error from the mean. Distances ($1000 \times$ scale) use visitation distribution \mathcal{D} from rollouts in the *train* environment of: a uniform random policy π_{unif} , an expert π^* and a **Mixture** of these policies. \mathcal{D}_S and \mathcal{D}_A are computed by marginalizing \mathcal{D} .

(a) 95% lower bound D^{LOW} of approximate distance.

| Reward | $1000 \times D_{\text{EPIC}}^{\text{LOW}}$ | | | $1000 \times D_{\text{NPEC}}^{\text{LOW}}$ | | | $1000 \times D_{\text{ERC}}^{\text{LOW}}$ | | |
|---------|--|---------|------|--|---------|-------|---|---------|------|
| | π_{unif} | π^* | Mix | π_{unif} | π^* | Mix | π_{unif} | π^* | Mix |
| Regress | 41.7 | 36.4 | 25.9 | 0.506 | 13.3 | 0.126 | 4.75 | 40.7 | 1.38 |
| Pref | 50.2 | 54.3 | 32.7 | 2.80 | 159 | 1.76 | 15.0 | 179 | 8.11 |
| AIRL SO | 484 | 599 | 393 | 673 | 2640 | 417 | 446 | 380 | 232 |
| AIRL SA | 544 | 614 | 388 | 804 | 1630 | 370 | 505 | 465 | 206 |

(b) Mean approximate distance \bar{D} . Results are the same as Table 2.

| Reward | $1000 \times \bar{D}_{\text{EPIC}}$ | | | $1000 \times \bar{D}_{\text{NPEC}}$ | | | $1000 \times \bar{D}_{\text{ERC}}$ | | |
|---------|-------------------------------------|---------|------|-------------------------------------|---------|-------|------------------------------------|---------|------|
| | π_{unif} | π^* | Mix | π_{unif} | π^* | Mix | π_{unif} | π^* | Mix |
| Regress | 41.9 | 36.5 | 25.9 | 0.519 | 14.9 | 0.140 | 4.78 | 40.9 | 1.39 |
| Pref | 50.5 | 54.4 | 32.9 | 2.99 | 204 | 1.78 | 15.0 | 180 | 8.15 |
| AIRL SO | 488 | 600 | 395 | 684 | 3550 | 426 | 448 | 382 | 234 |
| AIRL SA | 548 | 614 | 390 | 823 | 3030 | 376 | 506 | 467 | 208 |

(c) 95% upper bound D^{UP} of approximate distance.

| Reward | $1000 \times D_{\text{EPIC}}^{\text{UP}}$ | | | $1000 \times D_{\text{NPEC}}^{\text{UP}}$ | | | $1000 \times D_{\text{ERC}}^{\text{UP}}$ | | |
|---------|---|---------|------|---|---------|-------|--|---------|------|
| | π_{unif} | π^* | Mix | π_{unif} | π^* | Mix | π_{unif} | π^* | Mix |
| Regress | 42.2 | 36.5 | 26.0 | 0.535 | 16.8 | 0.162 | 4.80 | 41.1 | 1.40 |
| Pref | 50.9 | 54.5 | 33 | 3.16 | 240 | 1.80 | 15.1 | 181 | 8.19 |
| AIRL SO | 492 | 601 | 397 | 694 | 4420 | 436 | 450 | 384 | 235 |
| AIRL SA | 552 | 614 | 392 | 848 | 4660 | 385 | 508 | 469 | 209 |

(d) Relative 95% confidence interval $D^{\text{REL}} = \max\left(\frac{\text{Upper}}{\text{Mean}} - 1, 1 - \frac{\text{Lower}}{\text{Mean}}\right)$ in percent. The population mean is contained within $\pm D^{\text{REL}}\%$ of the sample mean in Table A.6b with 95% probability.

| Reward | $D_{\text{EPIC}}^{\text{REL}}\%$ | | | $D_{\text{NPEC}}^{\text{REL}}\%$ | | | $D_{\text{ERC}}^{\text{REL}}\%$ | | |
|---------|----------------------------------|---------|-------|----------------------------------|---------|------|---------------------------------|---------|-------|
| | π_{unif} | π^* | Mix | π_{unif} | π^* | Mix | π_{unif} | π^* | Mix |
| Regress | 0.662 | 0.0950 | 0.352 | 3.04 | 12.9 | 16.0 | 0.589 | 0.544 | 0.620 |
| Pref | 0.683 | 0.158 | 0.411 | 6.31 | 21.8 | 1.41 | 0.499 | 0.538 | 0.481 |
| AIRL SO | 0.875 | 0.115 | 0.522 | 1.60 | 25.8 | 2.37 | 0.449 | 0.504 | 0.621 |
| AIRL SA | 0.654 | 0.0331 | 0.397 | 3.15 | 53.9 | 2.34 | 0.382 | 0.445 | 0.540 |

A.3 Proofs

A.3.1 Background

Proposition 3.5. *The binary relation \equiv is an equivalence relation. Let $R_A, R_B, R_C : \mathcal{S} \times \mathcal{A} \times \mathcal{S} \rightarrow \mathbb{R}$ be bounded reward functions. Then \equiv is reflexive, $R_A \equiv R_A$; symmetric, $R_A \equiv R_B$ implies $R_B \equiv R_A$; and transitive, $(R_A \equiv R_B) \wedge (R_B \equiv R_C)$ implies $R_A \equiv R_C$.*

Proof. $R_A \equiv R_A$ since $R_A(s, a, s') = \lambda R_A(s, a, s') + \gamma \Phi(s') - \Phi(s)$ for all $s, s' \in \mathcal{S}$ and $a \in \mathcal{A}$ for $\lambda = 1 > 0$ and $\Phi(s) = 0$, a bounded potential function.

Suppose $R_A \equiv R_B$. Then there exists some $\lambda > 0$ and a bounded potential function $\Phi : \mathcal{S} \rightarrow \mathbb{R}$ such that $R_B(s, a, s') = \lambda R_A(s, a, s') + \gamma \Phi(s') - \Phi(s)$ for all $s, s' \in \mathcal{S}$ and $a \in \mathcal{A}$. Rearranging, we have:

$$R_A(s, a, s') = \frac{1}{\lambda} R_B(s, a, s') + \gamma \left(\frac{-1}{\lambda} \Phi(s') \right) - \left(\frac{-1}{\lambda} \Phi(s) \right).$$

Since $\frac{1}{\lambda} > 0$ and $\Phi'(s) = \frac{-1}{\lambda} \Phi(s)$ is a bounded potential function, it follows that $R_B \equiv R_A$.

Finally, suppose $R_A \equiv R_B$ and $R_B \equiv R_C$. Then there exists some $\lambda_1, \lambda_2 > 0$ and bounded potential functions $\Phi_1, \Phi_2 : \mathcal{S} \rightarrow \mathbb{R}$ such that for all $s, s' \in \mathcal{S}$ and $a \in \mathcal{A}$:

$$\begin{aligned} R_B(s, a, s') &= \lambda_1 R_A(s, a, s') + \gamma \Phi_1(s') - \Phi_1(s) \\ R_C(s, a, s') &= \lambda_2 R_B(s, a, s') + \gamma \Phi_2(s') - \Phi_2(s) \end{aligned}$$

Substituting the expression for R_B into the expression for R_C :

$$\begin{aligned} R_C(s, a, s') &= \lambda_2 (\lambda_1 R_A(s, a, s') + \gamma \Phi_1(s') - \Phi_1(s)) + \gamma \Phi_2(s') - \Phi_2(s) \\ &= \lambda_1 \lambda_2 R_A(s, a, s') + \gamma (\lambda_2 \Phi_1(s') + \Phi_2(s')) - (\lambda_2 \Phi_1(s) + \Phi_2(s)) \\ &= \lambda R_A(s, a, s') + \gamma \Phi(s') - \Phi(s), \end{aligned}$$

where $\lambda = \lambda_1 \lambda_2 > 0$ and $\Phi(s) = \lambda_2 \Phi_1(s) + \Phi_2(s)$ is bounded. Thus $R_A \equiv R_C$. \square

A.3.2 Equivalent-Policy Invariant Comparison (EPIC) pseudometric

Proposition 4.2 (The Canonically Shaped Reward is Invariant to Shaping). *Let $R : \mathcal{S} \times \mathcal{A} \times \mathcal{S} \rightarrow \mathbb{R}$ be a reward function and $\Phi : \mathcal{S} \rightarrow \mathbb{R}$ a potential function. Let $\gamma \in [0, 1]$ be a discount rate, and $\mathcal{D}_{\mathcal{S}}$ and $\mathcal{D}_{\mathcal{A}}$ be distributions over states \mathcal{S} and \mathcal{A} respectively. Let R' denote R shaped by Φ : $R'(s, a, s') = R(s, a, s') + \gamma \Phi(s') - \Phi(s)$. Then the canonically shaped R' and R are equal: $C_{\mathcal{D}_{\mathcal{S}}, \mathcal{D}_{\mathcal{A}}}(R') = C_{\mathcal{D}_{\mathcal{S}}, \mathcal{D}_{\mathcal{A}}}(R)$.*

Proof. Let $s, a, s' \in \mathcal{S} \times \mathcal{A} \times \mathcal{S}$. Then by substituting in the definition of R' and using linearity of expectations:

$$\begin{aligned} C_{\mathcal{D}_{\mathcal{S}}, \mathcal{D}_{\mathcal{A}}}(R')(s, a, s') &\triangleq R'(s, a, s') + \mathbb{E}[\gamma R'(s', A, S') - R'(s, A, S') - \gamma R'(S, A, S')] \\ &= (R(s, a, s') + \gamma \Phi(s') - \Phi(s)) + \mathbb{E}[\gamma R(s', a, S') + \gamma^2 \Phi(S') - \gamma \Phi(s')] \\ &\quad - \mathbb{E}[R(s, A, S') + \gamma \Phi(S') - \Phi(s)] - \mathbb{E}[\gamma R(S, A, S') + \gamma^2 \Phi(S') - \gamma \Phi(S)] \\ &= R(s, a, s') + \mathbb{E}[\gamma R(s', a, S') - R(s, A, S') - \gamma R(S, A, S')] \\ &\quad + (\gamma \Phi(s') - \Phi(s)) + \mathbb{E}[\Phi(s) - \gamma \Phi(s')] \\ &\quad + \mathbb{E}[\gamma^2 \Phi(S') - \gamma \Phi(S')] - \mathbb{E}[\gamma^2 \Phi(S') - \gamma \Phi(S)] \\ &= R(s, a, s') + \mathbb{E}[\gamma R(s', a, S') - R(s, A, S') - \gamma R(S, A, S')] \\ &\triangleq C_{\mathcal{D}_{\mathcal{S}}, \mathcal{D}_{\mathcal{A}}}(R)(s, a, s'), \end{aligned}$$

where the penultimate step uses $\mathbb{E}[\Phi(S')] = \mathbb{E}[\Phi(S)]$ since S and S' are identically distributed. \square

Lemma 4.5. *Let $a, b \in (0, \infty)$, $c, d \in \mathbb{R}$ and X, Y be random variables. Then it follows that $0 \leq D_{\rho}(aX + c, bY + d) = D_{\rho}(X, Y) \leq 1$.*

Proof. $D_\rho(aX + c, bY + d) = D_\rho(X, Y)$ immediate from $\rho(X, Y)$ invariant to positive affine transformations. Have $-1 \leq \rho(X, Y) \leq 1$, so $0 \leq 1 - \rho(X, Y) \leq 2$ thus $0 \leq D_\rho(X, Y) \leq 1$. \square

Lemma 4.4. *The Pearson distance D_ρ is a pseudometric.*

Proof. For a random variable V , define a standardized (zero mean and variance) version:

$$\hat{V} = \frac{V - \mathbb{E}[V]}{\sqrt{\mathbb{E}[(V - \mathbb{E}[V])^2]}}$$

The Pearson correlation coefficient on random variables X and Y is equal to the expected product of these standardized random variables:

$$\rho(X, Y) = \mathbb{E}[\hat{X}\hat{Y}].$$

Let X, Y and Z be random variables.

Identity. Have $\rho(X, X) = 1$, so $D_\rho(X, X) = 0$.

Symmetry. Have $\rho(X, Y) = \rho(Y, X)$ by commutativity of multiplication, so $D_\rho(X, Y) = D_\rho(Y, X)$.

Triangle Inequality. For any random variables A, B :

$$\begin{aligned} \mathbb{E}[(\hat{A} - \hat{B})^2] &= \mathbb{E}[\hat{A}^2 - 2\hat{A}\hat{B} + \hat{B}^2] \\ &= \mathbb{E}[\hat{A}^2 - 2\hat{A}\hat{B} + \hat{B}^2] \\ &= \mathbb{E}[\hat{A}^2] + \mathbb{E}[\hat{B}^2] - 2\mathbb{E}[\hat{A}\hat{B}] \\ &= 2 - 2\mathbb{E}[\hat{A}\hat{B}] \\ &= 2(1 - \rho(A, B)) \\ &= 4D_\rho(A, B)^2. \end{aligned}$$

So:

$$\begin{aligned} 4D_\rho(X, Z)^2 &= \mathbb{E}[(\hat{X} - \hat{Z})^2] \\ &= \mathbb{E}[(\hat{X} - \hat{Y} + \hat{Y} - \hat{Z})^2] \\ &= \mathbb{E}[(\hat{X} - \hat{Y})^2] + \mathbb{E}[(\hat{Y} - \hat{Z})^2] + 2\mathbb{E}[(\hat{X} - \hat{Y})(\hat{Y} - \hat{Z})] \\ &= 4D_\rho(X, Y)^2 + 4D_\rho(Y, Z)^2 + 8\mathbb{E}[(\hat{X} - \hat{Y})(\hat{Y} - \hat{Z})]. \end{aligned}$$

Since $\langle A, B \rangle = \mathbb{E}[AB]$ is an inner product over \mathbb{R} , it follows by the Cauchy-Schwarz inequality that $\mathbb{E}[AB] \leq \sqrt{\mathbb{E}[A^2]\mathbb{E}[B^2]}$. So:

$$\begin{aligned} D_\rho(X, Z)^2 &\leq D_\rho(X, Y)^2 + D_\rho(Y, Z)^2 + 2D_\rho(X, Y)D_\rho(Y, Z) \\ &= (D_\rho(X, Y) + D_\rho(Y, Z))^2. \end{aligned}$$

Taking the square root of both sides:

$$D_\rho(X, Z) \leq D_\rho(X, Y) + D_\rho(Y, Z),$$

as required. \square

Theorem 4.8. *Let $R_A, R'_A, R_B, R'_B : \mathcal{S} \times \mathcal{A} \times \mathcal{S} \rightarrow \mathbb{R}$ be reward functions such that $R'_A \equiv R_A$ and $R'_B \equiv R_B$. Then $0 \leq D_{\text{EPIC}}(R'_A, R'_B) = D_{\text{EPIC}}(R_A, R_B) \leq 1$.*

Proof. The result follows from D_ρ being a pseudometric. Let R_A, R_B and R_C be reward functions mapping from transitions $\mathcal{S} \times \mathcal{A} \times \mathcal{S}$ to real numbers \mathbb{R} .

Identity. Have:

$$\begin{aligned} D_{\text{EPIC}}(R_A, R_A) &= D_\rho(C_{\mathcal{D}_S, \mathcal{D}_A}(R_A)(S, A, S'), C_{\mathcal{D}_S, \mathcal{D}_A}(R_A)(S, A, S')) \\ &= 0, \end{aligned}$$

since $D_\rho(X, X) = 0$.

Symmetry. Have:

$$\begin{aligned} D_{\text{EPIC}}(R_A, R_B) &= D_\rho(C_{\mathcal{D}_S, \mathcal{D}_A}(R_A)(S, A, S'), C_{\mathcal{D}_S, \mathcal{D}_A}(R_B)(S, A, S')) \\ &= D_\rho(C_{\mathcal{D}_S, \mathcal{D}_A}(R_B)(S, A, S'), C_{\mathcal{D}_S, \mathcal{D}_A}(R_A)(S, A, S')) \\ &= D_{\text{EPIC}}(R_B, R_A), \end{aligned}$$

since $D_\rho(X, Y) = D_\rho(Y, X)$.

Triangle Inequality. Have:

$$\begin{aligned} D_{\text{EPIC}}(R_A, R_C) &= D_\rho(C_{\mathcal{D}_S, \mathcal{D}_A}(R_A)(S, A, S'), C_{\mathcal{D}_S, \mathcal{D}_A}(R_C)(S, A, S')) \\ &\leq D_\rho(C_{\mathcal{D}_S, \mathcal{D}_A}(R_A)(S, A, S'), C_{\mathcal{D}_S, \mathcal{D}_A}(R_B)(S, A, S')) \\ &\quad + D_\rho(C_{\mathcal{D}_S, \mathcal{D}_A}(R_B)(S, A, S'), C_{\mathcal{D}_S, \mathcal{D}_A}(R_C)(S, A, S')) \\ &= D_{\text{EPIC}}(R_A, R_B) + D_{\text{EPIC}}(R_B, R_C), \end{aligned}$$

since $D_\rho(X, Z) \leq D_\rho(X, Y) + D_\rho(Y, Z)$. \square

A.3.3 Nearest Point in Equivalence Class (NPEC) premetric

Proposition 5.3. (1) D_{L^p} is a metric in L^p space, where functions f and g are identified if $f = g$ almost everywhere on \mathcal{D} . (2) It is a pseudometric when f and g are identified if $f = g$ at all points.

Proof. (1) D_{L^p} is a metric in the L^p space since L^p is a norm in the L^p space, and $d(x, y) = \|x - y\|$ is always a metric. (2) As $f = g$ at all points implies $f = g$ almost everywhere, certainly $D_{L^p}(R, R) = 0$. Symmetry and triangle inequality do not depend on identity so still hold. \square

Proposition 5.5. D_{NPEC} is a premetric.

Proof. Let R_A, R_B be bounded reward functions on $\mathcal{S} \times \mathcal{A} \times \mathcal{S} \rightarrow \mathbb{R}$.

Respects identity: $D_{\text{NPEC}}(R_A, R_A) = 0$

If $D_{\text{NPEC}}^U(\text{Zero}, R_A) = 0$ then $D_{\text{NPEC}}(R_A, R_A) = 0$ as required. Suppose from now on that $D_{\text{NPEC}}(R_A, R_A) \neq 0$. It follows from prop 5.3 that $D_{L^p}(R_A, R_A) = 0$. Since $X \equiv X$, 0 is an upper bound for $D_{\text{NPEC}}^U(R_A, R_A)$. By prop 5.3 D_{L^p} is non-negative, so this is also a lower bound for $D_{\text{NPEC}}^U(R_A, R_A)$. So $D_{\text{NPEC}}^U(R_A, R_A) = 0$ and:

$$D_{\text{NPEC}}(R_A, R_A) = \frac{D_{\text{NPEC}}^U(R_A, R_A)}{D_{\text{NPEC}}^U(\text{Zero}, R_A)} = \frac{0}{D_{\text{NPEC}}^U(\text{Zero}, R_A)} = 0.$$

Well-defined: $D_{\text{NPEC}}(R_A, R_B) \geq 0$

By prop 5.3, it follows that $D_{L^p}(R, R_B) \geq 0$ for all reward functions $R : \mathcal{S} \times \mathcal{A} \times \mathcal{S}$. Thus 0 is a lower bound for $\{D_{L^p}(R, R_B) \mid R : \mathcal{S} \times \mathcal{A} \times \mathcal{S}\}$, and thus certainly a lower bound for $\{D_{L^p}(R, Y) \mid R \equiv X\}$ for any reward function X . Since the infimum is the *largest* lower bound, it follows that for any reward function X :

$$D_{\text{NPEC}}^U(X, R_B) \triangleq \inf_{R \equiv X} D_{L^p}(R, R_B) \geq 0.$$

In the case that $D_{\text{NPEC}}^U(\text{Zero}, R_B) = 0$, then $D_{\text{NPEC}}(R_A, R_B) = 0$ which is non-negative. From now on, suppose that $D_{\text{NPEC}}^U(\text{Zero}, R_B) \neq 0$. The quotient of a non-negative value with a positive value is non-negative, so:

$$D_{\text{NPEC}}(R_A, R_B) = \frac{D_{\text{NPEC}}^U(R_A, R_B)}{D_{\text{NPEC}}^U(\text{Zero}, R_B)} \geq 0. \quad \square$$

Note when D_{L^p} is a metric, then $D_{\text{NPEC}}(X, Y) = 0$ if and only if $X = Y$.

Proposition A.1. D_{NPEC} is not symmetric in the undiscounted case.

Proof. We will provide a counterexample showing that D_{NPEC} is not symmetric.

Choose the state space \mathcal{S} to be binary $\{0, 1\}$ and the actions \mathcal{A} to be the singleton $\{0\}$. Choose the visitation distribution \mathcal{D} to be uniform on $s \xrightarrow{0} s$ for $s \in \mathcal{S}$. Take $\gamma = 1$, i.e. undiscounted. Note that as the successor state is always the same as the start state, potential shaping has no effect on D_{direct} , so WLOG we will assume potential shaping is always zero.

Now, take $R_A(s) = 2s$ and $R_B(s) = 1$. Take $p = 1$ for the L^p distance. Observe that $D_{L^p}(\text{Zero}, R_A) = \frac{1}{2}(|0| + |2|) = 1$ and $D_{L^p}(\text{Zero}, R_B) = \frac{1}{2}(|1| + |1|) = 1$. Since potential shaping has no effect, $D_{\text{NPEC}}^U(\text{Zero}, R) = D_{L^p}(\text{Zero}, R)$ and so $D(\text{Zero}, R_A) = 1$ and $D(\text{Zero}, R_B) = 1$.

Now:

$$\begin{aligned} D_{\text{NPEC}}^U(R_A, R_B) &= \inf_{\lambda > 0} D_{L^p}(\lambda R_A, R_B) \\ &= \inf_{\lambda > 0} \frac{1}{2} (|\lambda| + |2\lambda - 1|) \\ &= \frac{1}{2}, \end{aligned}$$

with the infimum attained at $\lambda = \frac{1}{2}$. But:

$$\begin{aligned} D_{\text{NPEC}}^U(R_B, R_A) &= \inf_{\lambda > 0} D_{L^p}(\lambda R_B, R_A) \\ &= \inf_{\lambda > 0} \frac{1}{2} f(\lambda) \\ &= \frac{1}{2} \inf_{\lambda > 0} f(\lambda), \end{aligned}$$

where:

$$f(\lambda) = |\lambda| + |2 - \lambda|, \quad \lambda > 0.$$

Note that:

$$f(\lambda) = \begin{cases} 2 & \lambda \in (0, 2], \\ 2\lambda - 2 & \lambda \in (2, \infty). \end{cases}$$

So $f(\lambda) \geq 2$ on all of its domain, thus:

$$D_{\text{NPEC}}^U(R_B, R_A) = 1.$$

Consequently:

$$D_{\text{NPEC}}(R_A, R_B) = \frac{1}{2} \neq 1 = D_{\text{NPEC}}(R_B, R_A).$$

□

Proposition A.2 (Properties of D_{NPEC}^U). Let $R_A, R_B : \mathcal{S} \times \mathcal{A} \times \mathcal{S} \rightarrow \mathbb{R}$ be bounded reward functions, and $\lambda \geq 0$. Then D_{NPEC}^U :

- **Is invariant under \equiv in source:**
 $D_{\text{NPEC}}^U(R_A, R_B) = D_{\text{NPEC}}^U(R_B, R_B)$ if $R_A \equiv R_B$.
- **Invariant under scale-preserving \equiv in target:**
 $D_{\text{NPEC}}^U(R_A, R_A) = D_{\text{NPEC}}^U(R_A, R_B)$ if $R_A - R_B \equiv \text{Zero}$.
- **Scalable in target:**
 $D_{\text{NPEC}}^U(R_A, \lambda R_B) = \lambda D_{\text{NPEC}}^U(R_A, R_B)$.
- **Bounded:**
 $D_{\text{NPEC}}^U(R, R_B) \leq D_{\text{NPEC}}^U(\text{Zero}, R_B)$.

Proof. We will show each case in turn.

Invariance under \equiv in source

If $R_A \equiv R_B$, then:

$$\begin{aligned} D_{\text{NPEC}}^U(R_A, R_B) &\triangleq \inf_{R \equiv R_A} D_{L^p}(R, R_B) \\ &= \inf_{R \equiv R_B} D_{L^p}(R, R_B) \\ &\triangleq D_{\text{NPEC}}^U(R_B, R_B), \end{aligned}$$

since $R \equiv R_A$ if and only if $R \equiv R_B$ as \equiv is an equivalence relation.

Invariance under scale-preserving \equiv in target

If $R_A - R_B \equiv \text{Zero}$, then we can write $R_A(s, a, s') - R_B(s, a, s') = \gamma\Phi(s') - \Phi(s)$ for some potential function $\Phi : \mathcal{S} \rightarrow \mathbb{R}$. Then for any reward function R , since D is induced by a norm:

$$\begin{aligned} D_{L^p}(R, R_A) &\triangleq \mathbb{E}_{s, a, s' \sim \mathcal{D}} [D(R(s, a, s'), R_A(s, a, s'))] \\ &= \mathbb{E}_{s, a, s' \sim \mathcal{D}} [\|R(s, a, s') - R_A(s, a, s')\|] \\ &= \mathbb{E}_{s, a, s' \sim \mathcal{D}} [\|R(s, a, s') - (R_B(s, a, s') + \gamma\Phi(s') - \Phi(s))\|] \\ &= \mathbb{E}_{s, a, s' \sim \mathcal{D}} [\|(R(s, a, s') - \gamma\Phi(s') + \Phi(s)) - R_B(s, a, s')\|] \\ &= \mathbb{E}_{s, a, s' \sim \mathcal{D}} [D(R(s, a, s') - \gamma\Phi(s') + \Phi(s), R_B(s, a, s'))] \\ &\triangleq D_{L^p}(f(R), R_B), \tag{1} \end{aligned}$$

where $f(R)(s, a, s') = R(s, a, s') - \gamma\Phi(s') + \Phi(s)$. Crucially, note $f(R)$ is a bijection on the equivalence class $[R]$. Now, substituting this into the expression for NPEC premetric:

$$\begin{aligned} D_{\text{NPEC}}^U(R_A, R_A) &\triangleq \inf_{R \equiv R_A} D_{L^p}(R, R_A) \\ &= \inf_{R \equiv R_A} D_{L^p}(f(R), R_B) && \text{eq. 1} \\ &= \inf_{f(R) \equiv R_A} D_{L^p}(f(R), R_B) && f \text{ bijection on } [R] \\ &= \inf_{R \equiv R_A} D_{L^p}(R, R_B) && f \text{ bijection on } [R] \\ &\triangleq D_{\text{NPEC}}^U(R_A, R_B). \end{aligned}$$

Scalable in target First, note that D_{L^p} is absolutely scalable in both arguments:

$$D_{L^p}(\lambda R_A, \lambda R_B) \triangleq \mathbb{E}_{s, a, s' \sim \mathcal{D}} [D(\lambda R_A(s, a, s'), \lambda R_B(s, a, s'))] \tag{2}$$

$$= \mathbb{E}_{s, a, s' \sim \mathcal{D}} [\|\lambda R_A(s, a, s') - \lambda R_B(s, a, s')\|] \tag{3}$$

$$= \mathbb{E}_{s, a, s' \sim \mathcal{D}} [\|\lambda\| \|R_A(s, a, s') - R_B(s, a, s')\|] \quad \|\cdot\| \text{ absolutely scalable} \tag{4}$$

$$= |\lambda| \mathbb{E}_{s, a, s' \sim \mathcal{D}} [\|R_A(s, a, s') - R_B(s, a, s')\|] \tag{5}$$

$$\triangleq |\lambda| D_{L^p}(R_A, R_B). \tag{6}$$

Now, for $\lambda > 0$, applying this to NPEC premetric:

$$\begin{aligned} D_{\text{NPEC}}^U(R_A, \lambda R_B) &\triangleq \inf_{R \equiv R_A} D_{L^p}(R, \lambda R_B) \\ &= \inf_{R \equiv R_A} D_{L^p}(\lambda R, \lambda R_B) && R \equiv \lambda R \\ &= \inf_{R \equiv R_A} \lambda D_{L^p}(R, R_B) \\ &= \lambda \inf_{R \equiv R_A} D_{L^p}(R, R_B) \\ &\triangleq \lambda D_{\text{NPEC}}^U(R_A, R_B). \end{aligned}$$

In the case $\lambda = 0$, then:

$$\begin{aligned}
D_{\text{NPEC}}^U(R_A, 0) &\triangleq \inf_{R \equiv R_A} D_{L^p}(R, 0) \\
&= \inf_{R \equiv R_A} D_{L^p}\left(\frac{1}{2}R, 0\right) && R \equiv \frac{1}{2}R \\
&= \inf_{R \equiv R_A} \frac{1}{2}D_{L^p}(R, 0) \\
&= \frac{1}{2} \inf_{R \equiv R_A} D_{L^p}(R, 0) \\
&= \frac{1}{2}D_{\text{NPEC}}^U(R_A, 0).
\end{aligned}$$

Rearranging, we have:

$$D_{\text{NPEC}}^U(R_A, 0) = 0.$$

Boundedness

Suppose R_A is bounded by B : $|R_A(s, a, s')| \leq B$ for all $s, s' \in \mathcal{S}$ and $a \in \mathcal{A}$. Suppose the NPEC premetric $D_{\text{NPEC}}(0, R_B) = d$. Then for any $\epsilon > 0$, there exists some potential function $\Phi : \mathcal{S} \rightarrow \mathbb{R}$ such that the L^p of the potential shaping $R(s, a, s') \triangleq \gamma\Phi(s) - \Phi(s)$ from R_B satisfies:

$$D_{L^p}(R, R_B) \leq d + \epsilon. \quad (7)$$

Let $\lambda \in [0, 1]$. Define:

$$R'_\lambda(s, a, s') \triangleq \lambda R_A(s, a, s') + R(s, a, s'),$$

and:

$$f_\lambda(s, a, s') = D(R'_\lambda(s, a, s'), R(s, a, s')).$$

Note that:

$$\lim_{\lambda \rightarrow 0} R'_\lambda = R'_0 \text{ pointwise,}$$

and $R'_0 = R$. Since D is a metric it is continuous, and so:

$$\lim_{\lambda \rightarrow 0} f_\lambda = f_0 \text{ pointwise.}$$

Moreover, $f_0(s, a, s') = 0$ everywhere since $D(x, x) = 0$. Now:

$$\begin{aligned}
|f_\lambda(s, a, s')| &= D(R'_\lambda(s, a, s'), R(s, a, s')) \\
&= \|R'_\lambda(s, a, s') - R(s, a, s')\| \\
&= \|\lambda R_A(s, a, s')\| \\
&\leq \lambda B.
\end{aligned}$$

It follows by the bounded convergence theorem that:

$$\begin{aligned}
\lim_{\lambda \rightarrow 0^+} D_{L^p}(R'_\lambda, R) &= \lim_{\lambda \rightarrow 0^+} \mathbb{E}_{s, a, s' \sim \mathcal{D}} [f_\lambda(s, a, s')] \\
&= \mathbb{E}_{s, a, s' \sim \mathcal{D}} \left[\lim_{\lambda \rightarrow 0^+} f_\lambda(s, a, s') \right] \\
&= \mathbb{E}_{s, a, s' \sim \mathcal{D}} [f_0(s, a, s')] \\
&= 0.
\end{aligned}$$

So in particular, for any $\epsilon > 0$ there exists some $\lambda > 0$ such that:

$$D_{L^p}(R'_\lambda, R) \leq \epsilon. \quad (8)$$

Note that $R_A \equiv R'_\lambda$ for all $\lambda > 0$. So:

$$\begin{aligned}
D_{\text{NPEC}}(R_A, R_B) &\leq D_{L^p}(R'_\lambda, R_B) \\
&\leq D_{L^p}(R'_\lambda, R) + D_{L^p}(R, R_B) && \text{prop. 5.3} \\
&\leq \epsilon + (d + \epsilon) && \text{eq. 7 and eq. 8} \\
&= d + 2\epsilon.
\end{aligned}$$

Since $\epsilon > 0$ can be made arbitrarily small, it follows:

$$D_{\text{NPEC}}(R_A, R_B) \leq d. \quad (9)$$

□

Theorem 5.6. Let $R_A, R_A', R_B, R_B' : \mathcal{S} \times \mathcal{A} \times \mathcal{S} \rightarrow \mathbb{R}$ be reward functions such that $R_A \equiv R_A'$ and $R_B \equiv R_B'$. Then $0 \leq D_{\text{NPEC}}(R_A', R_B') = D_{\text{NPEC}}(R_A, R_B) \leq 1$.

Proof. Since $R_B' \equiv R_B$, we have $R_B' - \lambda R_B \equiv \text{Zero}$ for some $\lambda > 0$. By proposition A.2, D_{NPEC}^U is invariant under scale-preserving \equiv in target and scalable in target. That is, for any reward R :

$$D_{\text{NPEC}}^U(R, R_B') = D_{\text{NPEC}}^U(R, \lambda R_B) = \lambda D_{\text{NPEC}}^U(R, R_B). \quad (10)$$

In particular, $D_{\text{NPEC}}^U(\text{Zero}, R_B') = \lambda D_{\text{NPEC}}^U(\text{Zero}, R_B)$. As $\lambda > 0$, it follows that $D_{\text{NPEC}}^U(\text{Zero}, R_B') = 0 \iff D_{\text{NPEC}}^U(\text{Zero}, R_B) = 0$.

Suppose $D_{\text{NPEC}}^U(\text{Zero}, R_B) = 0$. Then $D_{\text{NPEC}}(R, R_B) = 0 = D_{\text{NPEC}}(R, R_B')$ for any reward R , so the result trivially holds. From now on, suppose $D_{\text{NPEC}}^U(\text{Zero}, R_B) \neq 0$.

By proposition A.2, D_{NPEC}^U is invariant to \equiv in source. That is, $D_{\text{NPEC}}^U(R_A, R_B) = D_{\text{NPEC}}^U(R_A', R_B)$, so:

$$D_{\text{NPEC}}(R_A', R_B) = \frac{D_{\text{NPEC}}^U(R_A', R_B)}{D_{\text{NPEC}}^U(\text{Zero}, R_B)} = \frac{D_{\text{NPEC}}^U(R_A, R_B)}{D_{\text{NPEC}}^U(\text{Zero}, R_B)} = D_{\text{NPEC}}(R_A, R_B).$$

By eq. (10):

$$D_{\text{NPEC}}(R_A, R_B') = \frac{\lambda D_{\text{NPEC}}^U(R_A, R_B)}{\lambda D_{\text{NPEC}}^U(\text{Zero}, R_B)} = \frac{D_{\text{NPEC}}^U(R_A, R_B)}{D_{\text{NPEC}}^U(\text{Zero}, R_B)} = D_{\text{NPEC}}(R_A, R_B).$$

Since D_{NPEC} is a premetric it is non-negative. By the boundedness property of proposition A.2, $D_{\text{NPEC}}^U(R, R_B) \leq D_{\text{NPEC}}^U(\text{Zero}, R_B)$, so:

$$D_{\text{NPEC}}(R_A, R_B) = \frac{D_{\text{NPEC}}^U(R_A, R_B)}{D_{\text{NPEC}}^U(\text{Zero}, R_B)} \leq 1. \quad \square$$

A.4 Direct Distance Variant of EPIC

Previously, we used Pearson distance to compare the canonicalized rewards. Pearson distance is naturally invariant to scaling. An alternative is to explicitly normalize the canonicalized rewards, and then compare them using any metric over functions.

Definition A.3 (Normalized Reward). Let R be a reward function mapping from transitions $\mathcal{S} \times \mathcal{A} \times \mathcal{S}$ to real numbers \mathbb{R} . Let $\|\cdot\|$ be some norm on the vector space of reward functions over the real field. Then the normalized R is:

$$R^N(s, a, s') = \frac{R(s, a, s')}{\|R\|}$$

Note that $(\lambda R)^N = R^N$ for any $\lambda > 0$ as norms are absolutely homogeneous.

We say a reward is *standardized* if it has been canonicalized and then normalized.

Definition A.4 (Standardized Reward). Let R be a reward function mapping from transitions $\mathcal{S} \times \mathcal{A} \times \mathcal{S}$ to real numbers \mathbb{R} . Then the standardized R is:

$$R^S = (C_{\mathcal{D}_S, \mathcal{D}_A}(R))^N.$$

Now, we can define a pseudometric based on the direct distance between the standardized rewards.

Definition A.5 (Direct Distance Standardized Reward). Let \mathcal{D} be some visitation distribution over transitions $s \xrightarrow{a} s'$. Let \mathcal{D}_S and \mathcal{D}_A be some distributions over states \mathcal{S} and \mathcal{A} respectively. Let

S, A, S' be random variables jointly sampled from \mathcal{D} . The Direct Distance Standardized Reward pseudometric between two reward functions R_A and R_B is the direct distance between their standardized versions over \mathcal{D} :

$$D_{\text{DDSR}}(R_A, R_B) = \frac{1}{2} D_{L^p} (R_A^S(S, A, S'), R_B^S(S, A, S')),$$

where the norm used for direct distance is the same norm used for normalization in R^N .

For brevity, we omit the proof that D_{DDSR} is a pseudometric, but this follows from D_{L^p} being a pseudometric in a similar fashion to theorem 4.7. Note it additionally is invariant to equivalence classes, similarly to EPIC.

Theorem A.6. Let $R_A, R_{A'}, R_B$ and $R_{B'}$ be reward functions mapping from transitions $\mathcal{S} \times \mathcal{A} \times \mathcal{S}$ to real numbers \mathbb{R} such that $R_A \equiv R_{A'}$ and $R_B \equiv R_{B'}$. Then:

$$0 \leq D_{\text{DDSR}}(R_{A'}, R_{B'}) = D_{\text{DDSR}}(R_A, R_B) \leq 1.$$

Proof. The invariance under the equivalence class follows from R^S being invariant to potential shaping and scale in R . The non-negativity follows from D_{L^p} being a pseudometric. The upper bound follows from the rewards being normalized to norm 1 and the triangle inequality:

$$\begin{aligned} D_{\text{DDSR}}(R_A, R_B) &= \frac{1}{2} \|R_A^S - R_B^S\| \\ &\leq \frac{1}{2} (\|R_A^S\| + \|R_B^S\|) \\ &= \frac{1}{2} (1 + 1) \\ &= 1. \end{aligned} \quad \square$$

Since both DDSR and EPIC are pseudometrics and invariant on equivalent rewards, it is interesting to consider the connection between them. In fact, under the L^2 norm with \mathcal{D} chosen to be i.i.d. samples from the joint distribution $\mathcal{D}_S \times \mathcal{D}_A \times \mathcal{D}_S$, then DDSR recovers EPIC. First, we will show that canonical shaping centers the reward functions.

Lemma A.7 (The Canonically Shaped Reward is Mean Zero). Let R be a reward function mapping from transitions $\mathcal{S} \times \mathcal{A} \times \mathcal{S}$ to real numbers \mathbb{R} . Then:

$$\mathbb{E}[C_{\mathcal{D}_S, \mathcal{D}_A}(R)(S, A, S')] = 0.$$

Proof. Let X, U and X' be random variables that are independent of S, A and S' but identically distributed.

$$\begin{aligned} \mathbb{E}[C_{\mathcal{D}_S, \mathcal{D}_A}(R)(S, A, S')] &= \mathbb{E}[R(S, A, S') + \gamma R(S', U, X') - R(S, U, X') - \gamma R(X, U, X')] \\ &= \mathbb{E}[R(S, A, S')] + \gamma \mathbb{E}[R(S', U, X')] - \mathbb{E}[R(S, U, X')] - \gamma \mathbb{E}[R(X, U, X')] \\ &= \mathbb{E}[R(S, U, X')] + \gamma \mathbb{E}[R(X, U, X')] - \mathbb{E}[R(S, U, X')] - \gamma \mathbb{E}[R(X, U, X')] \\ &= 0, \end{aligned}$$

where the penultimate step follows since A is identically distributed to U , and S' is identically distributed to X' and therefore to X . \square

Recall from the proof of lemma 4.4 that:

$$\begin{aligned} D_\rho(U, V) &= \frac{1}{2} \sqrt{\mathbb{E}[(\hat{U} - \hat{V})^2]} \\ &= \frac{1}{2} \|\hat{U} - \hat{V}\|_2, \end{aligned}$$

where $\|\cdot\|_2$ is the L^2 norm (treating the random variables as functions on a measure space) and \hat{U} is a centered (zero-mean) and rescaled (unit variance) random variable. By lemma A.7, the canonically

shaped reward functions are already centered under the joint distribution $\mathcal{D}_S \times \mathcal{D}_A \times \mathcal{D}_S$, and normalization by the L^2 norm also ensures they have unit variance. Consequently:

$$\begin{aligned}
D_{\text{EPIC}}(R_A, R_B) &= D_\rho(C_{\mathcal{D}_S, \mathcal{D}_A}(R_A)(S, A, S'), C_{\mathcal{D}_S, \mathcal{D}_A}(R_B)(S, A, S')) \\
&= \frac{1}{2} \left\| C_{\mathcal{D}_S, \mathcal{D}_A}(R_A)(S, A, S') - C_{\mathcal{D}_S, \mathcal{D}_A}(R_B)(S, A, S') \right\|_2 \\
&= \frac{1}{2} \|R_A^S(S, A, S') - R_B^S(S, A, S')\|_2 \\
&= \frac{1}{2} D_{L^p}(R_A^S(S, A, S'), R_B^S(S, A, S')) \\
&= D_{\text{DDSR}}(R_A, R_B).
\end{aligned}$$